

Morphotectonic characteristics, distribution and probable genesis of bathymetric highs off southwest coast of India

C.M. Bijesh^{1,2}, P. John Kurian^{1,*}, V. Yatheesh³, Abhishek Tyagi¹, D. Twinkle¹

¹ National Centre for Antarctic and Ocean Research, Vasco da Gama, Goa, 403804, India

² Department of Marine Sciences, Goa University, Taleigao Plateau, Goa 403206, India

³ CSIR - National Institute of Oceanography, Dona Paula, Goa 403004, India

Abstract

The western continental margin of India and the adjacent deep ocean basins were formed by break-up and separation among India, Seychelles and Madagascar since the Late Cretaceous. The initial India-Madagascar separation and the subsequent India-Seychelles separation are believed to have been caused by the Marion hotspot at ~90 Ma and the Réunion hotspot at ~68.5 Ma, respectively. These geodynamic events resulted in the formation of several bathymetric highs that probably represent imprints of these volcanic events. In the present study these bathymetric high features were mapped comprehensively to understand their morphotectonic characteristics, using a fresh set of multibeam bathymetry, sea-surface gravity and magnetic anomalies, complemented by the available multichannel seismic reflection sections. A high-resolution bathymetric map of the southwestern continental margin of India and the adjoining deep offshore regions has been generated to decipher detailed morphological configuration and distribution of prominent undersea bathymetric features. We also carried out detailed morphometric analysis of these features to deduce the morphological parameters. A total of 33 individual bathymetric high features were identified and classified as seamounts, hills, knolls, guyots and plateaus based on the standardization of undersea feature names published by Intergovernmental Oceanographic Commission (IOC) and International Hydrographic Organization (IHO) in 2013. Multichannel seismic reflection, sea-surface gravity and magnetic data were used to describe the sub-seafloor configuration and qualitative interpretation of the geophysical signatures associated with the bathymetric highs. Interpretation of the multichannel seismic reflection sections suggest that some of these identified features are extrusive in nature, while others are intrusive. These features are associated with characteristic gravity highs superimposed over regional negative anomalies and complex negative and positive magnetic anomalies. The study results suggest that the genesis of the bathymetric highs mapped in the study area could be attributed to the hotspot volcanism, caused by the Marion or Réunion hotspots. We infer that the features in the southwestern continental margin of India closer to the Alleppey-Trivandrum Terrace Complex might have been created by the Marion hotspot volcanism, while those in the Laccadive Basin and eastern sector of the Laccadive Plateau might have been formed by Réunion hotspot volcanism.

Keywords: Seafloor Morphology, Hotspot Volcanism, Laccadive Basin, Laccadive Plateau

* Corresponding author

E-mail address: john@ncaor.gov.in; kurianjohn@gmail.com (P. John Kurian)

Tel: +91 832 2525570; Fax: +91 832 2520877

1. Introduction

Bathymetric high features are important submarine physiographic features, which have been a subject of interest in geophysical, geological, oceanographic and biological aspects. Detailed investigations of the bathymetric features are important because such studies can provide vital clues for understanding the evolution of deep ocean basins and the adjacent continental margins as well as identification of economically important mineral deposits. Research focused on the morphological and geophysical aspects of the bathymetric high features were widely conducted in the world ocean (Menard, 1964; Smith and Jordan., 1988; Wessel, 2001; Wessel et al., 2010; Harris et al., 2014). Various hypotheses were proposed for the formation of these bathymetric high features, mainly, hotspot activity, ridge-hotspot interaction, ridge parallel faulting, off axis volcanism and propagating fracture (Fornari et al., 1984; Duncan and Clague, 1985; Fornari et al., 1988; Shen et al., 1993; Clague et al., 2000; Clouard et al., 2003; Das et al., 2007).

In the Indian Ocean, extensive studies of geomorphologic features were carried out in the Central Indian Basin (Kodagali, 1989, 1992, 1998; Mukhopadhyay and Khadge, 1990; Mukhopadhyay and Batiza, 1994; Das et al., 2005, 2007; Iyer, 2009; Iyer et al., 2012), however, such studies of morphological features are comparatively sparse in the Western Indian Ocean except a few in the Arabian Sea (Bhattacharya and Subrahmanyam, 1991; Bhattacharya et al., 1994; Mukhopadhyay et al., 2008; Rao et al., 2010). Bhattacharya and Subrahmanyam (1991) carried out detailed geophysical study over the Sagar Kanya Seamount (Fig. 1) in the Arabian Basin and provided crustal configuration and probable genesis for this seamount. Bhattacharya et al. (1994) mapped a seamount chain in the Laxmi Basin, consisting of the Raman Seamount, Panikkar Seamount and Wadia Guyot (Fig. 1). Subsequently, Mukhopadhyay et al. (2008) and Rao et al. (2010) studied bathymetric highs in the mid continental slope region of the southwestern continental margin of India (SWCMI). However, such detailed geomorphologic studies were not undertaken in the Laccadive Basin and the adjacent areas (Fig. 1), which consists of several prominent bathymetric highs. In the present study, we attempt first to map these bathymetric features in the Laccadive Basin, eastern part of the Laccadive Plateau and the southwestern continental margin of India and then to discuss their distribution and probable mode of emplacement.

2. Tectonic framework

The study area (Fig. 1) mainly consists of the southwestern continental margin of India, the Laccadive Basin and the eastern part of the Laccadive Plateau, located between 6°N and 16°N latitudes. The southwestern continental margin of India clearly shows the presence of an anomalous terrace like feature in the mid continental slope region off Trivandrum. Yatheesh et al. (2013)

referred this feature as the Alleppey-Trivandrum Terrace Complex, which mainly consists a smaller northerly terrace, the Alleppey Terrace, and a larger southerly terrace, the Trivandrum Terrace (Yatheesh et al., 2006). The western boundary of the Alleppey-Trivandrum Terrace Complex is marked by an escarpment, the Chain-Kairali Escarpment, which is defined by a ~500 km-long feature with a sharp drop in the bathymetry (Yatheesh et al., 2013). The region located west of the Chain-Kairali Escarpment and east of the Laccadive Plateau is the Laccadive Basin, which is a triangular shaped basin created due to divergence between India and the Laccadive Plateau (Bhattacharya and Chaubey, 2001; Bhattacharya and Yatheesh, 2015). The nature of crust underlying the Laccadive Basin is still equivocal. Based on the presence of rotated fault blocks representing half grabens, Chaubey et al. (2002a) suggested that the Laccadive Basin represents a failed rift consisting of stretched continental crust intermingled with volcanics. Considering the presence of seaward dipping reflectors (SDRs) west of the Laccadive Plateau and based on gravity modeling, Ajay et al. (2010) inferred that the Laccadive Basin is underlain by thinned continental crust. Yatheesh et al. (2013), based on gravity modeling, demonstrated that the Laccadive Basin region could be underlain either by a much thinned continental crust or by an anomalously thick oceanic crust. The Laccadive Plateau is the northernmost segment of the Laccadive-Chagos Ridge, which is slightly arcuate, elongated feature extending about 2500 km between 14°N and 9°S latitudes. Various views exist for the genesis of the Laccadive-Chagos Ridge, such as, a leaky transform fault (Fisher et al., 1971; Sclater and Fisher, 1974), hotspot trail (Whitmarsh, 1974a; Duncan, 1981; Morgan, 1981), a composite structural elements of various origin (Avraham and Bunce, 1977) and crack propagation (Sheth, 2005). Though the hotspot trail genesis appears to have broader acceptance for the genesis of the Laccadive-Chagos Ridge as a whole, there are several observations, which strongly suggest that the Laccadive Plateau is a continental sliver (Bhattacharya and Yatheesh, 2015 and references therein). The Laccadive Plateau area has a complex block-faulted basement structure, constituting system of grabens, half grabens and single normal faults, which are grouped into a rift system, referred as the Cannanore Rift System (DGH, 2014).

3. Data and Methodology

The main data used in the present study comprise of sea-surface magnetic, gravity and multibeam bathymetry data, acquired by National Centre for Antarctic and Ocean Research (NCAOR), Goa, India, during 2007 to 2016 onboard various research vessels (Table 1). The multibeam bathymetry data was collected using Atlas Hydrosweep DS System (onboard *MV Akademik Boris Petrov*), SeaBeam 3012 Multibeam System (onboard *ORV SagarKanya*) and Reson SeaBat 7150 (onboard *MV MGS Sagar*). The Atlas Hydrosweep DS System was operated at a

frequency of 15.5 kHz with maximum angular coverage of 120°. The SeaBeam 3012, with a maximum angular coverage of 140°, was operated at a frequency of 12 kHz. The Reson SeaBat 7150 was operated in dual-frequency (12 kHz and 24 kHz), depending on the depth range. The measured depth values are corrected for variation of sound velocity in seawater by collecting sound velocity profiles in real time. This raw multibeam dataset was processed using Caris Hips & Sips software package in which all the datasets were merged together. Finally, manual de-spiking and qualitative filtering were applied to minimize the erroneous depth soundings. The processed data was then extracted in ASCII format and prepared a bathymetric grid with 250 m spatial resolution using Generic Mapping Tools (GMT). Mobile Gravimeter Chekan - AM was used to acquire the sea-surface gravity data and was reduced to gravity anomalies by applying normal and Eötvös corrections. The total field magnetic data was collected using Marine Magneto Explorer Pro magnetometer. These data were reduced to residual magnetic anomalies by applying International Geomagnetic Reference Field (IGRF) for the corresponding epoch. Both gravity and magnetic data were acquired with ~30m spatial resolution along the track and using these data, 1x1km grids were generated for the preparation of 2D gravity and magnetic anomaly maps. To understand the sub-seafloor characteristics of the various features, we used multichannel seismic reflection data (along the profiles SWC-01, SWC-03 and SWC-07), collected by Directorate General of Hydrocarbon (DGH), India, as well as two published (Whitmarsh, 1974b; Rao et al., 2010) seismic sections. The locations of sea-surface gravity, magnetic and seismic reflection profiles used to characterize various bathymetric features in the present study are given in Fig. 2 and Supplementary Fig.S1.

4. Results and Discussion

4.1 Seafloor morphology from multibeam bathymetry data

The updated bathymetric maps (Fig. 2 and Supplementary Fig. S1) of the study region covers an area of ~2,34,000 km². This high resolution bathymetric map shows the presence of 33 distinct bathymetric highs with varying size and height. We classify these seafloor features into different categories such as seamounts, hills, knolls, guyots and plateaus, following the classification scheme of International Hydrographic Organization (IOC-IHO, 2013). We inferred the morphological characteristics of these features and derived their morphometric parameters. Locations of the identified features and their morphometric characteristics are shown in Fig. 2 and Fig. 3, respectively. The derived morphometric parameters, which mainly consist of height, basal area, basal width, slope angle, flatness and height-width ratio, are detailed in Table 2. In this section, we provide a detailed description of geomorphology of the identified bathymetric features and their morphometric characteristics.

4.1.1 Seamounts

Seamounts are distinct generally equi-dimensional elevation greater than 1000 m above the surrounding relief as measured from the deepest isobath that surrounds most of the feature (IOC-IHO, 2013). From the updated bathymetric map of the study area, 14 seamounts (S1 to S14, as shown in Fig. 2 and Table 2), with varying height of 1045-2260 m from the surrounding seafloor, were identified. Among these, 12 seamounts (S2 to S11 and S13 to S14) are located in the eastern sector of the Laccadive Plateau and the adjacent region of the Laccadive Basin, while two seamounts (S1 and S12) are located close to the southwestern continental slope of India. Most of these features are with single peak along the summit, but seamounts S9, S12 and S14 are characterized by four, two and three peaks, respectively. Seamount S5, a conical feature, has least basal extent ($\sim 55 \text{ km}^2$) and seamount S11 has maximum basal extent ($\sim 694 \text{ km}^2$). The 3D bathymetric images and corresponding contour maps of two representative seamounts, S11 and S2 are presented in Fig. 4. (See Supplementary Fig. S2 for bathymetric image of all the other seamounts). Seamount S11, which has maximum height (2260 m), shows (Fig. 3) significantly large slope angle and basal width but less flatness. The plot of basal width against height for the seamounts shows that height increases (1000 to 1500 m) roughly with increasing basal width (7 to 17 km) for the seamounts (Fig. 3).

4.1.2 Hills and Knolls

Hills are distinct elevations generally of irregular shape, less than 1000 m above the surrounding relief as measured from the deepest isobath that surrounds most of the feature (IOC-IHO, 2013). On the other hand, Knolls are distinct elevations with a rounded profile less than 1000 m above the surrounding relief, as measured from the deepest isobath that surrounds most of the feature (IOC-IHO, 2013). The bathymetric map reveals the presence of clearly distinguishable 8 hills (H1 to H8) and 3 knolls (K1 to K3). These identified features are presented in Fig. 2 and their morphometric details are given in Table 2. Most of the hills and knolls are characterized by an increase in basal width and slope angle against increasing height (Fig. 3). The hills H1 to H5 and H8 are situated in relatively flat seafloor. The basal depth of hills H1 to H5 ranges between 1800-2000 m, while the basal depth of H8 is about 2750 m. These hills exhibit basal extents varying between 20.65 km^2 (H3) and 350 km^2 (H8), with varying height-width (H-W) ratio between 0.028 and 0.247. Three knolls, with basal depth ranging 1400-1800 m, were identified in the Laccadive Basin, with varying heights (310-940 m) and areal extents ($25\text{-}100 \text{ km}^2$). The 3D bathymetric image of a representative hill (H1) and knoll (K1) along with the contour maps are presented in Fig. 5 to describe the characteristic signatures of hills and knolls mapped in the study area. The bathymetric images of other hills and knolls are given in Supplementary figs. S3 and S4, respectively.

4.1.3 Guyots and Plateaus

Guyots are seamounts with comparatively smooth flat top and plateaus are large, relatively flat elevations that are higher than the surrounding relief with one or more relatively steep sides (IOC-IHO, 2013). The study area contains two guyots, which are located in relatively flat seafloor close to the eastern flank of the Laccadive Plateau (Fig. 2). These guyots G1 and G2, whose basal depths are about 1800 m, show basal extent of 96 km² and 330 km², with flatness of 0.330 to 0.510, respectively (Fig. 3 and Table 2). The 3D bathymetric and the contour maps of guyots G1 and G2 are presented in Fig. 6. From the bathymetric map, we also identify six plateaus, Pt1 to Pt6 in the study area (Fig. 2). All the plateaus, except Pt6 are situated in the southwestern continental slope of India, while the plateau Pt5 is located in the Laccadive Basin. The plateaus in the continental slope exhibit different basal depths in the landward and seaward sides of these features. The basal depths for plateaus given in Table 2 represent those measured in the landward direction. These plateaus possess basal extent ranging from 123-1172 km² and flatness varying from 0.350-0.625 (Table 2). All plateaus exhibit moderate to steep sloping flanks, showing gully patterns over both the flanks. The 3D bathymetric images as well as color-coded contour maps of two representative plateaus, Pt1 and Pt2 are presented in Fig. 7 and the other plateaus are shown in Supplementary Fig. S5.

4.2 Sub-seafloor configuration from seismic reflection data

We used three multichannel and two single channel seismic sections (Fig. 8) to depict sub-seafloor configuration of the selected bathymetric features considered in the present study. The seismic sections SWC-01, SWC-03, SWC-07, AB and CD (Fig. 2) cut across the bathymetric high features S12, S7, H4, Pt1, and H7, respectively. Some of these features (Pt1, H7 and S12) are located in the continental slope region, while others (H4 and S7) are located in the deep sea basin. The multichannel seismic image of the hill H4 (Fig. 8a) and seamount S7 (Fig. 8b) show that the flanks of these features are steep and the sediments are nearly absent on top of them. This observation suggests that both these features might represent volcanic extrusives, with a basement high piercing through the sediment surface. On the other hand, the multichannel seismic image of the seamount S12 depict (Fig. 8c) a basement high associated with bulging of thick sediment layers (~2.5s TWT) on top of it, suggesting the presence of a subsurface intrusive. The single channel seismic section (Fig. 8d) across the plateau Pt1 shows that only a thin layer of the sediments (~0.4s TWT) exists on top of this ~20 km-wide bathymetric and basement highs. This feature, located in the continental slope region, was earlier identified by Rao et al. (2010) and they reported that the lower half of the flanks is covered mostly by slump sediments. The hill H7 represents a bathymetric feature with steep flanks (Fig. 8e), suggesting a volcanic extrusive. This feature represents the same bathymetric high

identified by Yatheesh et al. (2013) in the Chain-Kairali Escarpment domain in the southwestern continental margin of India.

4.3 Gravity and magnetic signatures

The free-air gravity anomalies and magnetic anomalies of the selected representative bathymetric high features are presented in Fig. 9 as images, contours and profiles to analyze their characteristics. The free-air gravity anomalies corresponding to all the features (presented in Fig. 9) are highly correlated with the topography, with an observed maximum corresponding to their summit. These anomalies decrease along the flanks of the features and get superimposed on the gravity signature of the surrounding flat seafloor. The hill H1 is characterized by a broader gravity anomaly with its maximum ($\sim -25\text{mGal}$) over its summit (Fig. 9a). The gravity anomaly at the summit of seamount S2 is $\sim -5\text{mGal}$ and its base is defined by the -50mGal contour (Fig. 9b). The highest magnitude of free-air gravity anomaly, among all the features presented in Fig. 9, is observed over the central part of plateau Pt3, reaching up to $\sim 20\text{mGal}$, with a magnitude of $\sim -70\text{mGal}$ at the base of the feature (Fig. 9c). The seamount S12 is described by free-air gravity anomalies of $\sim 15\text{mGal}$ for the summit and $\sim -40\text{mGal}$ for its base (Fig. 9d). The hill H7 corresponds to a nearly N-S trending gravity high with free-air gravity anomaly magnitudes of $\sim 15\text{mGal}$ over the summit and $\sim -35\text{mGal}$ at the base (Fig. 9e). The plateau Pt6 is represented as an E-W trending gravity high with $\sim 5\text{mGal}$ at summit and $\sim -30\text{mGal}$ at its base (Fig. 9f).

The northernmost region of Hill H1 is associated with an E-W trending negative magnetic anomaly with maximum intensity of -60nT and the southernmost region of this feature is characterized by a N-S trending positive magnetic anomaly with a maximum intensity of 130nT (Fig. 9a). The seamount S2 is characterized by a relatively broader magnetic anomaly with two peaks, one located closer to the northern flank and the other one located at the western flank of the seamount S2 (Fig. 9b). The intensity of this magnetic anomaly, trending nearly NNW-SSE, gradually decreases towards southern and eastern flanks of the seamount with a sharp change in magnetic intensity from 90nT to 60nT from the base of the seamount to the adjacent flat seafloor. The magnetic anomaly over plateau Pt3 exhibits a nearly circular pattern (Fig. 9c) with an observed maximum intensity corresponding to the foot of the western flank ($\sim 270\text{nT}$). The eastern part of the plateau Pt3 displays negative anomaly with an apparent intensity of $\sim 30\text{nT}$, which gradually increases westward and northward from the summit of the plateau. The seamount S12 exhibit a relatively flat signature of magnetic anomaly with an intensity of $\sim 100\text{nT}$, with a gradual increase in intensity towards southwest and a decrease in intensity towards north in its southwestern and northern extremities, respectively (Fig. 9d). The northernmost flank of the hill H7 coincides with a positive magnetic

anomaly peak of $\sim 170\text{nT}$, with a gradual decrease in intensity towards the south (Fig. 9e). The Plateau Pt6 is characterized by two negative magnetic anomalies, located on the northern and southern parts of the seamount, with intensities up to $\sim 380\text{nT}$ and $\sim 440\text{nT}$, respectively (Fig. 9f). The negative magnetic anomaly in the south coincides with the southern flank of the plateau, while those in the north are located on the northernmost region of the plateau summit. These two negative magnetic anomalies, trending nearly WNW-SSE, are divided by a zone of magnetic anomalies with maximum intensity of $\sim 260\text{nT}$.

4.4 Probable genesis of bathymetric highs

The updated plate tectonic evolution model of the Arabian Sea (Bhattacharya and Yatheesh, 2015) suggests that the western continental margin of India was formed by the rifting and subsequent drifting among India, Seychelles and Madagascar, along with the adjacent microcontinental slivers of the Laxmi Ridge and the Laccadive Plateau. Among these, the first episode was separation of India-Laxmi Ridge-Seychelles block from Madagascar, believed to have been caused by the Marion hotspot. The evidence to this inference comes from the existence of $\sim 85\text{-}92$ Ma volcanics from the western side of India (Valsangkar et al., 1981; Radhakrishna et al., 1994, 1999; Torsvik et al., 2000; Anil Kumar et al., 2001; Pande et al., 2001; Melluso et al., 2009; Radhakrishna and Joseph, 2012; Ram Mohan et al., 2016) and the eastern side of Madagascar (Storey et al., 1995; Torsvik et al., 2000). The second episode was separation of Seychelles-Laxmi Ridge block from India, which is considered to have been initiated by oldest pulse of Réunion hotspot (at ~ 68.5 Ma) as evidenced from the existence of ~ 68.5 Ma old volcanics located north of the main Deccan Flood Basalt province (Basu et al., 1993). During this period, a break-up occurred also between the Laccadive Plateau and India. At around $65\text{-}66$ Ma, the bulk of the Deccan Flood Basalt was emplaced on the Indian mainland with a large fraction of its activity during chron 29R (Courtillot et al., 1988), under the influence of the Réunion hotspot. Subsequently, the third episode of the break-up between Seychelles and Laxmi Ridge-India block occurred shortly before 62.5 Ma, coinciding with the formation of Ghatkopar-Powai tholeiitic basalt (Pande et al., 2017) and emplacement of Raman-Panikkar-Wadia seamount chain in the Laxmi Basin (Bhattacharya and Yatheesh, 2015; Pande et al., 2017). Evidence to this comes from the oldest magnetic anomalies (chron 28ny) inferred from the conjugate Arabian and Eastern Somali basins (Miles and Roest, 1993; Chaubey et al., 2002b), formed by seafloor spreading along the Carlsberg Ridge. The spreading along the Carlsberg Ridge continued with the northward motion of Indian plate over the Réunion hotspot and this motion caused the formation of the Laccadive-Chagos Ridge, which mainly consists of the Laccadive Plateau, Maldive Ridge and the Chagos Bank, along with the relatively deep saddle-like features.

The genesis of the bathymetric highs in the oceanic regions are generally explained in terms of hotspot activity, ridge-hotspot interaction, ridge parallel faulting, off-axis volcanism and propagating fracture, depending on the respective geological settings (Das et al., 2007 and references therein). The main geodynamic events occurred in the vicinity of our study area are the Marion and Réunion hotspots volcanism. Therefore, we attempt to provide a reasonable explanation for the genesis of the bathymetric highs in terms of hotspot volcanism. The bathymetric highs in the study area mainly falls in two domains, those located either in the continental slope of India or in the Laccadive Basin and the adjacent part of the Laccadive Plateau. The bathymetric features in the continental slope region are the plateaus Pt1, Pt2, Pt3, Pt4 and Pt6, hills H6 and H7, knoll K1, and seamount S12. The features, hills H6 and H7, seamount S12 and plateaus Pt4 and Pt6 are located over the Chain-Kairali Escarpment, which represents the western boundary of the thinned continental crust of the Alleppey-Trivandrum Terrace Complex. The Chain-Kairali Escarpment is interpreted (Yatheesh et al., 2013) to represent the transform boundary formed due to the gliding between India and Madagascar during the initial stages of India-Madagascar separation, caused by the Marion hotspot volcanism. Therefore, we believe that the bathymetric features located in the relatively southern region of Alleppey-Trivandrum Terrace Complex were created by the Marion hotspot volcanism (e.g. H-7, showing the characteristics of an extrusive body in Fig. 8e).

The plateaus Pt1, Pt2 and Pt3 and knoll K1 are located relatively north and some of these features (plateaus Pt1 and Pt3) were interpreted by Rao et al. (2010) to represent continental slivers and horst structures formed during stretching and faulting along the southwestern continental margin of India, implying India-Madagascar break-up. However, we observe that these features located in the relatively northern part of the study area are very close to the Réunion hotspot track (Fig. 10) and therefore one can equally argue the genesis of these features to Réunion hotspot volcanism as well as India-Madagascar rifting, caused by the Marion hotspot volcanism. Fig. 10 also shows that the Réunion hotspot track is very close to the eastern part of the Laccadive Plateau and therefore, we are tempted to attribute the genesis of these bathymetric highs in the Laccadive Basin and the Laccadive Plateau to the Réunion hotspot volcanism. Since the effect of the hotspot can go over several hundreds of kilometers distance (Tolan et al., 1989; Storey et al., 1995), such an interpretation is reasonable even if the referred features in the Laccadive Basin are located not over the hotspot track exactly. This suggestion on the effect of hotspot to a larger area is valid in the case of Sagar Kanya Seamount (Bhattacharya and Subrahmanyam, 1991) in the Arabian Sea. This seamount, which is inferred to have been formed by Réunion hotspot, is nearly 200 km away from the Réunion hotspot track (Fig. 10).

5. Summary and Conclusion

We carried out detailed geophysical investigations of bathymetric high features in the Laccadive Basin and the adjacent areas to understand their distribution, morphometry, geophysical characteristics and probable genesis. The updated bathymetric map of the study area highlights 33 bathymetric high features, consisting of 14 seamounts, 8 hills, 3 knolls, 2 guyots and 6 plateaus. Majority of the identified seamounts are located in the Laccadive Basin and the eastern sector of the Laccadive Plateau. Most of these seamounts are with single peak, but a few seamounts show multiple peaks. Morphometric analysis of these seamounts shows that height of the seamount increases roughly with increasing basal width. Morphology of the identified hills and knolls suggest a characteristic increase in basal width and slope angle against increasing height. We identified two adjacent guyots, located in relatively flat seafloor close to the eastern flank of the Laccadive Plateau. Most of the plateaus identified in the study area are located in the western continental slope of India and they exhibit moderate to steep sloping flanks, showing gully pattern on both the flanks. We analyzed sub-seafloor configuration of the selected bathymetric features using seismic reflection sections. The inferred basement configuration suggests that some of the bathymetric features might represent volcanic extrusives while others might represent basement highs associated with bulging of sediment layers over the subsurface volcanic intrusive. The sea-surface gravity signatures of the selected features suggest a characteristic relatively high gravity anomaly superimposed over a regional negative anomaly. This relative gravity high corresponds to the summit area of the bathymetric high and this gravity anomaly reduces along its flanks. The magnetic anomalies over the bathymetric high features exhibit complex behavior. Both negative and positive magnetic anomalies are observed over the features, superimposed over the regional magnetic signatures.

The study area is located very close to the southwestern continental margin of India, which was formed by the India-Seychelles-Madagascar break-up. The updated plate tectonic evolution model for the Arabian Sea suggests that the break-up between India and Madagascar occurred at ~90 Ma, believed to have been caused by the Marion hotspot, and then Seychelles-India break-up occurred at ~68.5 Ma, possibly caused by the earliest pulse of the Réunion hotspot (Bhattacharya and Yatheesh, 2015). We attempted to provide a reasonable answer for the genesis of the bathymetric features in the study area, under the constraints of this tectonic setting. Majority of these features appears to have caused by the hotspot volcanism, however, at present it is not possible to conclude whether these bathymetric highs are related to the Marion hotspot volcanism or Réunion hotspot volcanism. Based on the proximity of this region to the St. Mary Islands and the Ezhimala Igneous Complex, which are considered to be a product of the Marion hotspot, we consider that the

bathymetric highs located in the southwestern continental slope of India were formed by the Marion hotspot volcanism. But, the bathymetric features in the Laccadive Basin and eastern Laccadive Plateau are in the proximity of the Réunion hotspot track and therefore we attribute the genesis of these bathymetric features to the Réunion hotspot volcanism. However, detailed geochronological, paleomagnetic and geochemical investigations of the volcanic rocks collected from these identified features need to be carried out for the validation of the genesis proposed in the present study.

Acknowledgement

The authors are grateful to the Director, National Centre for Antarctic and Ocean Research (NCAOR), Goa and Director, CSIR – National Institute of Oceanography (CSIR-NIO), Goa, for their encouragement and support to carry out this work. The authors are also thankful to Ministry of Earth Sciences (MoES), New Delhi for their financial support through the EEZ Programme and EEZ Advisory Committee for permission to publish this work. This study forms a part of the PhD work of CMB at Goa University. We are indebted to the two anonymous reviewers for their careful review of the manuscript and valuable comments. We are grateful to Prof. Andrew James Plater, Editor, for editorial handling of the manuscript. We gratefully acknowledge the support received from the shipboard scientific party, officers and crew members of all the cruises of the EEZ Programme conducted onboard *Akademic Boris Petrov*, *ORV SagarKanya* and *MGS Sagar*. Directorate General of Hydrocarbons, New Delhi is thanked for providing the multichannel seismic reflection sections used in the present study. Figures were drafted with GMT (Wessel and Smith, 1995) and *SURFER*(www.goldensoftware.com). This is NCAOR contribution number xxxx and NIO contribution number xxxx.

Figure Captions:

Figure 1	Generalized map of the southwestern continental margin of India and the adjoining deep offshore regions showing the major tectonic features and geographic extent of the study area. Black dotted lines are selected (500, 1000, 2000, 3000 and 3500 m) isobaths from GEBCO digital data set (IOC-IHO-BODC, 2003). R: Raman Seamount; P: Panikkar Seamount; W: Wadia Guyot; S:SagarKanya Seamount; LP: Laccadive Plateau; PB: Padua Bank; MdR: Maldive Ridge; CKE: Chain Kairali Escarpment; ATTC: Alleppey-Trivandrum Terrace Complex; LR: Laxmi Ridge; LB: Laxmi Basin; StM: St. Mary Islands; EI: Ezhimala Igneous Complex.
Figure 2	The updated high resolution bathymetric map of the study area, showing the locations of the bathymetric high features identified in the present study. White lines represent locations of the seismic reflection sections presented in Figure 8. Black lines represent locations of sea-surface bathymetry, gravity and magnetic profiles presented in Figure 9 (profile plots).Black cross marks on these lines represent the extent of the profiles shown in Figure 9. Labels to the bathymetric high features are as in Table 2.
Figure 3	Plots of (a) height versus basal width (Wb), (b) height versus slope angle, (c) height versus flatness and (d)height versus H-W ratio of identified bathymetric high features. Morphometric details are given in Table 2.
Figure 4	Three-dimensional images (a and b) and the contour maps at 100 m interval (c and d) of the representative seamounts in the study area (Seamounts S2 and S11).
Figure 5	Three-dimensional images (a and b) and the contour maps at 100 m interval (c and d) of the representative hills and knolls in the study area (Hill H1 and Knoll K1).
Figure 6	Three-dimensional image (a) and the contour map at 100 m interval (b) of the representative Guyots G1 and G2 in the study area.
Figure 7	Three-dimensional images (a and b) and the contour maps at 100 m interval (c and d) of the representative plateaus in the study area (Plateaus Pt1 and Pt2).
Figure 8	Seismic reflection sections across (a) Hill H4; (b) Seamount S7; (c) Seamount

	S12; (d) Plateau Pt1; and (e) Hill H7. Locations of these sections are given in Figure 2 as white lines and in Supplementary Figure S1 as pink lines.
Figure 9	Maps of the gravity and magnetic anomalies along with the stacked bathymetry, gravity and magnetic profiles across selected features (a) Hill H1; (b) Seamount S2; (c) Plateau Pt3; (d) Seamount S12; (e) Hill H7; (f) Plateau Pt6. The black contours represent the isobaths at 200 m interval, used to depict the extent of the bathymetric features. The white lines on the gravity image represents gravity anomaly contours in 5 mGal interval and those in the magnetic image represents magnetic anomaly contours in 30nT interval. The locations of the stacked bathymetry, gravity and magnetic profiles segments within the grey dotted lines are shown as black thick lines in the gravity and magnetic images. FAA: Free-air gravity anomaly; MA: Magnetic anomaly.
Figure 10	Generalized bathymetric map (GEBCO isobaths) of the study area showing locations and distribution of the bathymetric features identified in the present study. The thick black line connecting the black solid circles represents the Réunion hotspot track computed based on Müller et al. (1993). The numbers given to the solid black circles represent the ages in million years (Ma). Other details are as in Figure 1.

Table Captions

Table 1	Details of cruises from which marine geophysical data have compiled for the present study.
Table 2	Morphometric details of the bathymetric high features identified in the study area. Locations of the features are shown in Figure 2.

References

- Ajay, K. K., Chaubey, A. K., Krishna, K. S., Rao, D. G., Sar, D., 2010. Seaward dipping reflectors along the SW continental margin of India: Evidence for volcanic passive margin. *Journal of Earth System Science* 119(6), 803–813.
- Anil Kumar, Pande, K., Venkatesan, T.R., Bhaskar Rao, Y.J., 2001. The Karnataka Late Cretaceous dykes as products of the Marion hotspot at the Madagascar-India breakup event: evidence from $^{40}\text{Ar}/^{39}\text{Ar}$ geochronology and geochemistry. *Geophysical Research Letters* 28 (14), 2715-2718.
- Avraham, Z.B., Bunce, E.T., 1977. Geological study of the Chagos-Laccadive Ridge, Indian Ocean. *Journal of Geophysical Research* 82, 1295-1305.
- Basu, A.R., Renne, P.R., Dasgupta, D.K., Teichmann, F., Poreda, R.J., 1993. Early and late igneous pulses and high ^3He plume origin for the Deccan Flood Basalts. *Science* 261, 902-906.
- Bhattacharya, G. C., Subrahmanyam, V., 1991. Geophysical study of a seamount located on the continental margin of India. *Geo-Marine Letters* 11(2), 71–78.
- Bhattacharya, G.C., Chaubey, A.K., 2001. Western Indian Ocean - A glimpse of the tectonic scenario. In: Sengupta R., Desa E. (Eds.) *The Indian Ocean - A Perspective*, Vol 2. Oxford & IBH, pp. 691-729.
- Bhattacharya, G.C., Murty, G.P.S, Srinivas, K., Chaubey, A.K., Sudhakar, T., Nair, R.R., 1994. Swath bathymetric investigation of the seamounts located in Laxmi Basin, Eastern Arabian Sea. *Marine Geodesy* 17, 169-182.
- Bhattacharya, G.C., Yatheesh, V., 2015. Plate-tectonic evolution of the deep ocean basins adjoining the western continental margin of India - a proposed model for the early opening scenario, In: Mukherjee, S. (Ed.), *Petroleum Geoscience: Indian Contexts*. Springer, pp. 1-61.
- Chaubey, A. K., Rao, D. G., Srinivas, K., Ramprasad, T., Ramana, M. V, Subrahmanyam, V., 2002a. Analyses of multichannel seismic reflection, gravity and magnetic data along a regional profile across the central-western continental margin of India. *Marine Geology* 182, 303-323.
- Chaubey, A.K., Dymant, J., Bhattacharya, G.C., Royer, J.Y., Srinivas, K., Yatheesh, V., 2002b. Paleogene magnetic isochrons and palaeo-propagators in the Arabian and Eastern Somali basins, NW Indian Ocean. In: Clift, P.D., Croon, D., Gaedicke, C., Craig, J. (Eds.), *The Tectonic and Climatic Evolution of the Arabian Sea Region*, Geological Society, London, Special Publication 195, pp. 71-85.
- Clague, D. A., Reynolds, J. R., Davis, A. S., 2000. Near-ridge seamount chains in the northeastern Pacific Ocean. *Journal of Geophysical Research-Solid Earth* 105, 16541–16561.
- Clouard, V., Bonneville, A., Gillot, P.-Y., 2003. The Tarava Seamounts: a newly characterized hotspot chain on the South Pacific Super swell. *Earth and Planetary Science Letters* 207, 117–130.
- Courtillot, V., Feraud, G., Maluski, H., Vandamme, D., Moreau, M.G., Besse, J., 1988. Deccan flood basalts and the Cretaceous/ Tertiary boundary. *Nature* 333, 843-846.
- Das, P., Iyer, S. D., Kodagali, V. N., 2007. Morphological characteristics and emplacement mechanism of the seamounts in the Central Indian Ocean Basin. *Tectonophysics* 443(1–2), 1–18.
- Das, P., Iyer, S. D., Kodagali, V. N., Krishna, K. S., 2005. Distribution and Origin of Seamounts in the Central Indian Ocean Basin. *Marine Geodesy* 28(3), 259–269.

- DGH, 2014. Directorate General of Hydrocarbons (DGH), Noida, India web page: Kerala Konkan Basin (accessed 29.10.14),<http://www.dghindia.org/15.aspx>.
- Duncan, R.A., 1981. Hotspots in the Southern Oceans - an absolute frame of reference for the motion of the Gondwana continents. *Tectonophysics* 74, 29-42.
- Duncan, R.A., Clague, D.A., 1985. Pacific plate motion recorded by linear volcanic chains. In: Nairn, A.E.M., Stehli, F.G., Uyeda, S. (Eds.), *The Ocean Basins and Margins*, Vol. 7A. Plenum, New York, pp. 89–112.
- Fisher, R. L., Sclater, J. G., McKenzie, D. P., 1971. Evolution of the Central Indian Ridge, Western Indian Ocean. *Geological Society of America Bulletin* 82, 553-562.
- Fornari, D.J., Perfit, M.R., Allen, J.F., Batiza, R., Haymon, R., Ryan, W.B.F., Smith, T., Simkin, T., Luckman, M.A., 1988. Seamounts as windows into the mantle process: structural and geochemical studies of the Lamont seamounts. *Earth and Planetary Science Letters* 89, 63–83.
- Fornari, D.J., Ryan, W.B.F., Fox, P.J., 1984. The evolution of craters and calderas on young seamounts: insight from sea MARC 1 and Sea Beam sonar surveys of a small seamount group near the axis of the East Pacific Rise at $\sim 10^\circ$ N. *Journal of Geophysical Research* 89, 11069–11083.
- Harris, P. T., Macmillan-Lawler, M., Rupp, J., Baker, E. K., 2014. Geomorphology of the oceans. *Marine Geology* 352, 4–24.
- IOC-IHO, 2013. Standardization of undersea feature names. Publication B-6, Edition 4.1.0, 18p.
- IOC-IHO-BODC, 2003. Centenary Edition of the GEBCO Digital Atlas. CD-ROM on Behalf of the Intergovernmental Oceanographic Commission and the International Hydrographic Organization as Part of the General Bathymetric Chart of the Oceans, British Oceanographic Data Centre, Liverpool, UK.
- Iyer, S.D., 2009. Seamounts- their formation, mineral deposits, biodiversity and atmospheric oxygen. *Geo-Spectrum Interface* 4, 33-36.
- Iyer, S.D., Mehta, C.M., Das, P., Kalangutkar, N.G., 2012. Seamounts - characteristics, formation, mineral deposits and biodiversity. *Geologica Acta* 10(3), 295-308.
- Kodagali V N., 1989. Morphometric Studies on a part of Central Indian Ocean. *Journal of Geological Society of India* 33, 547-555.
- Kodagali, V. N., 1992. Morphologic investigation of uncharted seamount from central Indian Basin revisited with multibeam sonar system. *Marine Geodesy* 15, 47–56.
- Kodagali, V.N., 1998. A pair of seamount chains in the Central Indian Basin, identified from multibeam mapping. *Marine Geodesy* 21(2), 147-158.
- Melluso, L., Sheth, H.C., Mahoney, J.J., Morra, V., Petrone, C.M., Storey, M., 2009. Correlations between silicic volcanic rocks of the St. Mary's Islands (southwestern India) and eastern Madagascar: implications for Late Cretaceous India Madagascar reconstructions. *Journal of Geological Society, London* 166, 283-294.
- Menard, H.W., 1964. *Marine Geology of the Pacific*. New York. McGraw-Hill Book Company, 271p.
- Miles P.R., Roest, W.R., 1993. Earliest seafloor spreading magnetic anomalies in the north Arabian Sea and the ocean-continent transition. *Geophysical Journal International* 115, 1025-1031
- Morgan W.J., 1981. Hotspot tracks and the opening of the Atlantic and Indian Oceans. In: Emiliani (Ed.) *The Sea*, Vol 7. Wiley Interscience New York, pp. 443-487.

- Mukhopadhyay, R., Batiza, R., 1994. Basinal seamounts and seamount chains of the Central Indian Ocean: Probable near-axis origin from a fast-spreading Ridge. *Marine Geophysical Researches* 16, 303-314.
- Mukhopadhyay, R., Khadge, N.H., 1990. Seamounts in the Central Indian Ocean Basin: indicators of the Indian plate movement. *Proceedings of the Indian Academy of Sciences (Earth and Planetary Sciences)* 99, 357-365.
- Mukhopadhyay, R., Rajesh, M., De, S., Chakraborty, B., Jauhari, P., 2008. Structural highs on the western continental slope of India: Implications for regional tectonics. *Geomorphology* 96(1-2), 48-61.
- Müller, D. R., Royer, J.-Y., Lawver, A. L., 1993. Revised plate motions relative to the hotspots from combined Atlantic and Indian Ocean hotspot tracks. *Geology* 21,275-278.
- Pande K., Sheth, H.C., Bhutani, R., 2001. $^{40}\text{Ar} - ^{39}\text{Ar}$ age of the St. Mary's Islands volcanics, southern India: record of India - Madagascar break-up on the Indian subcontinent. *Earth and Planetary Science Letters* 193, 39-46.
- Pande, K., Yatheesh, V., Sheth, H., 2017. $^{40}\text{Ar}/^{39}\text{Ar}$ dating of the Mumbai tholeiites and Panvel flexure: intense 62.5 Ma onshore-offshore Deccan magmatism during India-Laxmi Ridge-Seychelles breakup. *Geophysical Journal International* 210, 1160-1170.
- Radhakrishna, T., Dallmeyer, R. D., Joseph, M., 1994. Paleomagnetism and $^{36}\text{Ar}/^{40}\text{Ar}$ vs $^{39}\text{Ar}/^{40}\text{Ar}$ isotope correlation ages of dyke swarms in Central Kerala, India: tectonic implications. *Earth and Planetary Science Letters* 121, 213-226.
- Radhakrishna, T., Joseph, M., 2012. Geochemistry and paleomagnetism of Late Cretaceous mafic dikes in Kerala, southwest coast of India in relation to large igneous provinces and mantle plumes in the Indian Ocean region. *Geological Society of America Bulletin* 124 (1/2), 240-255.
- Radhakrishna, T., Maluski, H., Mitchell, J.G., Joseph, M., 1999. $^{40}\text{Ar}/^{39}\text{Ar}$ and K/Ar geochronology of the dykes from the south Indian granulite terrain. *Tectonophysics* 304, 109-129.
- Ram Mohan, M., Shaji, E., Satyanarayanan, M., Santosh, M., Tsunogae, T., Yang, Q. Y., DhanilDev, S. G., 2016. The Ezhimala Igneous Complex, southern India: Possible imprint of Late Cretaceous magmatism within rift setting associated with India-Madagascar separation. *Journal of Asian Earth Sciences* 121, 56-71.
- Rao, D. G., Paropkari, A. L., Krishna, K. S., Chaubey, A. K., Ajay, K. K., Kodagali, V. N., 2010. Bathymetric highs in the mid-slope region of the western continental margin of India- Structure and mode of origin. *Marine Geology* 276(1-4), 58-70.
- Sclater, J. G., Fisher, R. L., 1974. The evolution of the east central Indian Ocean. *Geological Society of America Bulletin* 85,683-702.
- Shen, Y., Scheirer, D.S., Forsyth, D.W., Macdonald, K.C., 1993. Two forms of volcanism: implications for mantle flow and off-axis crustal production on the west flank of the southern East Pacific Rise. *Journal of Geophysical Research* 98, 17875-17889.
- Sheth, H.C., 2005. From Deccan to Reunion: No trace of a mantle plume. In: Foulger, G.R., Natland, J.H., Presnall, D.C., Anderson, D.L. (Eds.) *Plates, Plumes, and Paradigms*, Special Paper 388. Geological Society of America, pp. 477-501.
- Smith, D.K., Jordan, T.H., 1988. Seamount statistics in the Pacific Ocean. *Journal of Geophysical Research* 93, 2899-2918.

- Storey, M, Mahoney, J.J., Saunders, A.D., Duncan, R.A., Kelley, S.P., Coffin, M.F., 1995. Timing of hotspot related volcanism and the breakup of Madagascar and India. *Science* 267 (5199), 852-855.
- Tolan, T.L., Reidel, S.P., Beeson, M.H., Anderson, J.L., Fecht, K.R., Swanson, D.A., 1989. Revisions to the estimates of the areal extent and volume of the Columbia River Basalt Group. In: Reidel, S.P., Hooper, P.R. (Eds.), *Volcanism and Tectonism in the Columbia River Flood-Basalt Province*. Geological Society of America Special Paper 239, pp. 1-20.
- Torsvik, T.H., Tucker, R.D., Ashwal, L.D., Carter, L.M., Jamtveit, V., Vidyadharan, K.T., Venkataramana, P., 2000. Late cretaceous India - Madagascar fit and timing of breakup related magmatism. *Terra Nova*, 12, 220-224.
- Valsangkar A.B., Radhakrishnamurthy, C., Subbarao, K.V., Beckinsale, R.D., 1981. Paleomagnetism and Potassium-Argon age studies of acid igneous rocks from the St. Mary Islands. *Geological Society of India* 3, 265-275.
- Wessel, P., 2001. Global distribution of seamounts inferred from gridded Geosat/ERS-1 altimetry. *Journal of Geophysical Research* 106, 19431-19441.
- Wessel, P., Sandwell, D.T., Kim, S.S., 2010. The global seamount census. *Oceanography* 23, 24-33.
- Wessel, P., Smith, W.H.F., 1995. New version of the Generic Mapping Tools released. *EOS Transactions, American Geophysical Union*, p. 329.
- Whitmarsh, R.B., 1974a. Some aspects of plate tectonics in the Arabian Sea. In: *Initial Reports of the Deep Sea Drilling Project*, 23, 527-535, US Govt. Printing Office, Washington.
- Whitmarsh, R.B., 1974b. Appendix V. Geophysical Appendix, in *Initial Reports of the Deep Sea Drilling Project*, 23, 1159-1171, US Govt. Printing Office, Washington.
- Yatheesh, V., Bhattacharya, G.C., Mahender, K., 2006. The terrace like feature in the mid-continental slope region off Trivandrum and a plausible model for India–Madagascar juxtaposition in immediate pre-drift scenario. *Gondwana Research* 10, 179-185.
- Yatheesh, V., Kurian, P. J., Bhattacharya, G. C., Rajan, S., 2013. Morphotectonic architecture of an India-Madagascar breakup related anomalous submarine terrace complex on the southwest continental margin of India. *Marine and Petroleum Geology* 46, 304–318.

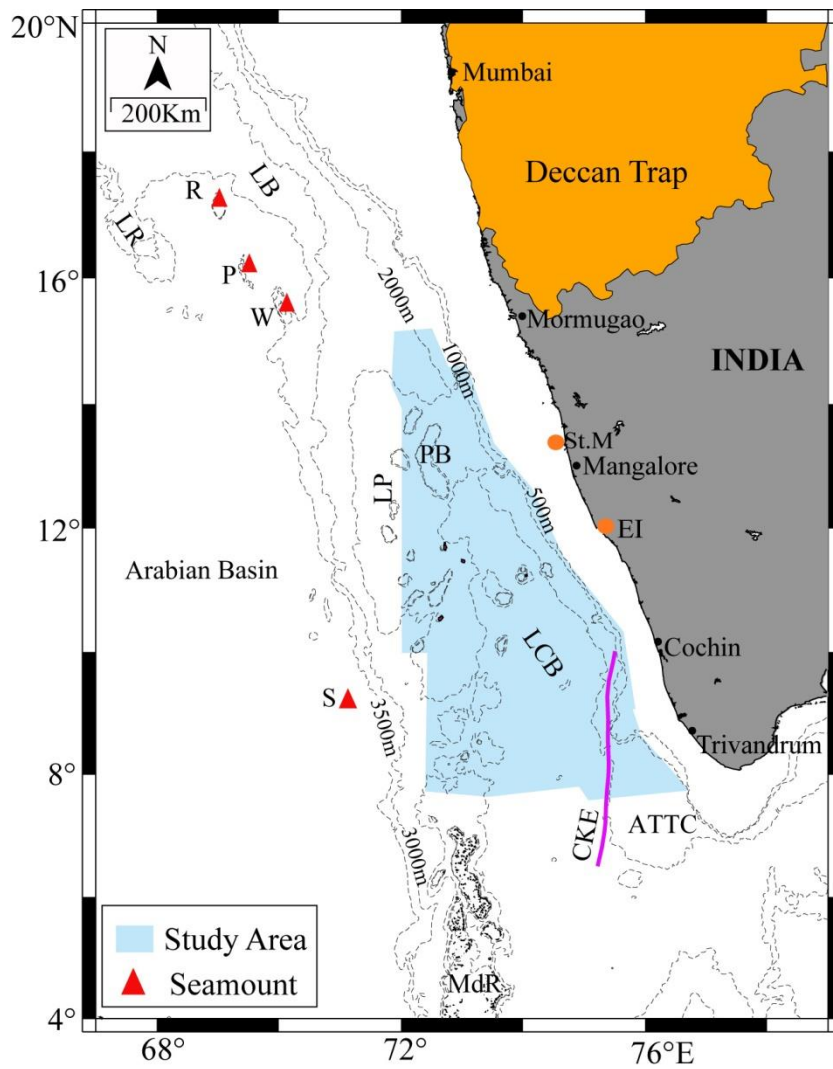


Figure 1

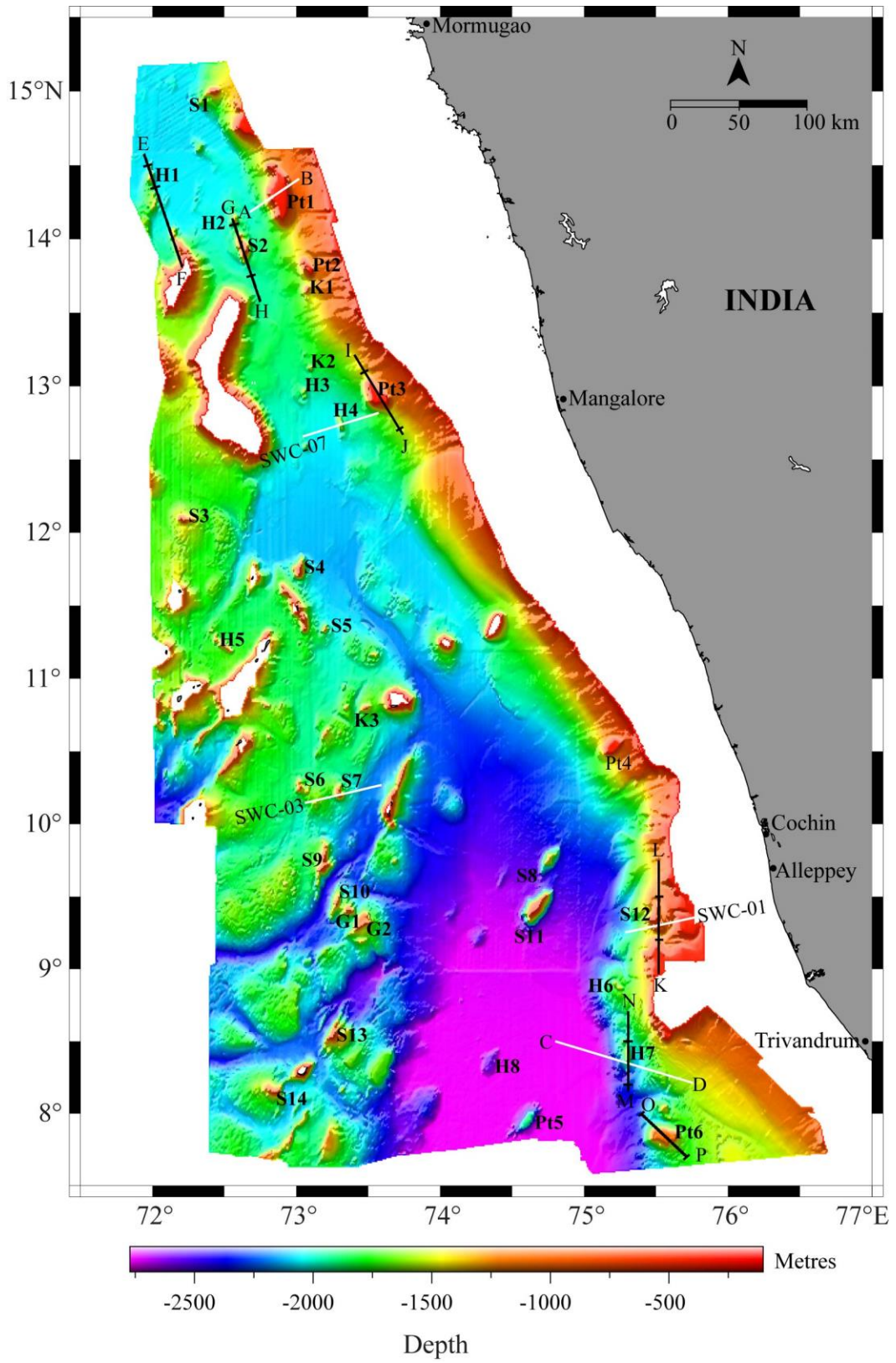


Figure 2

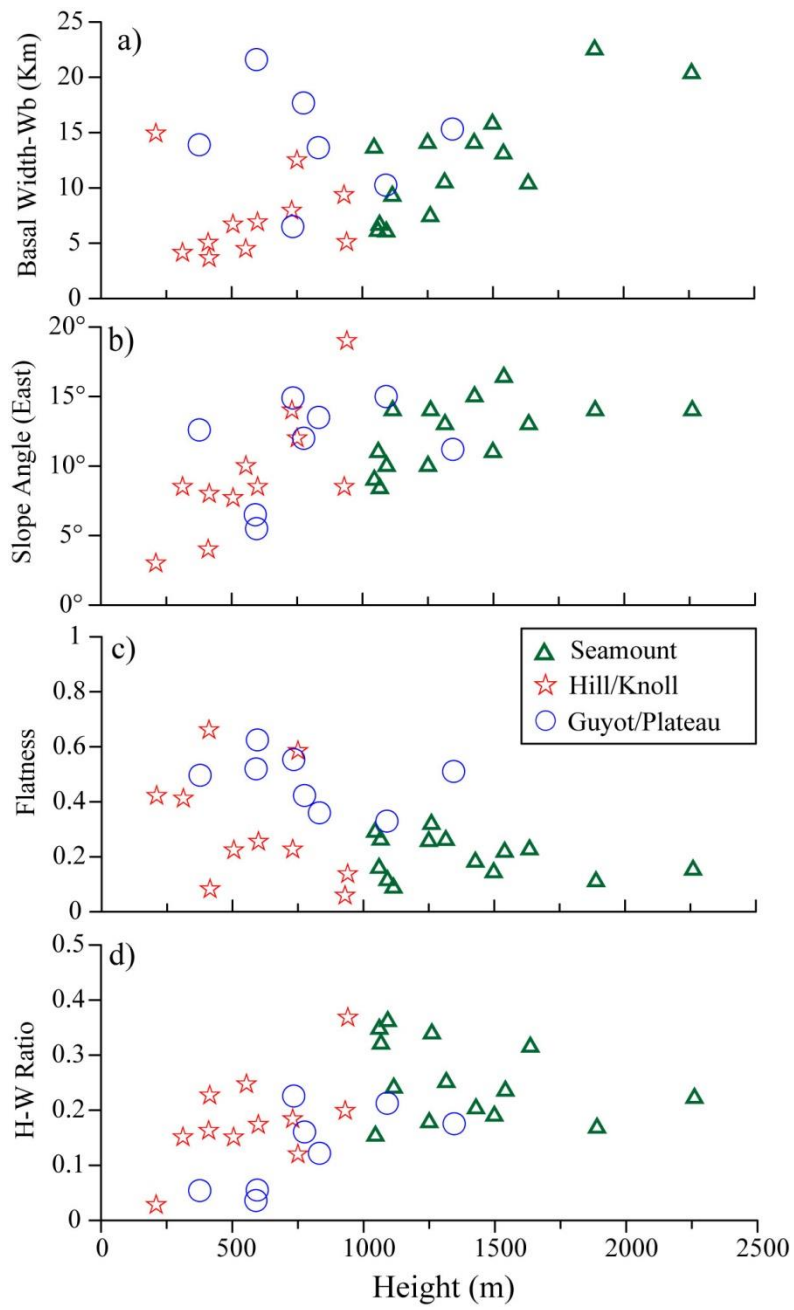


Figure 3

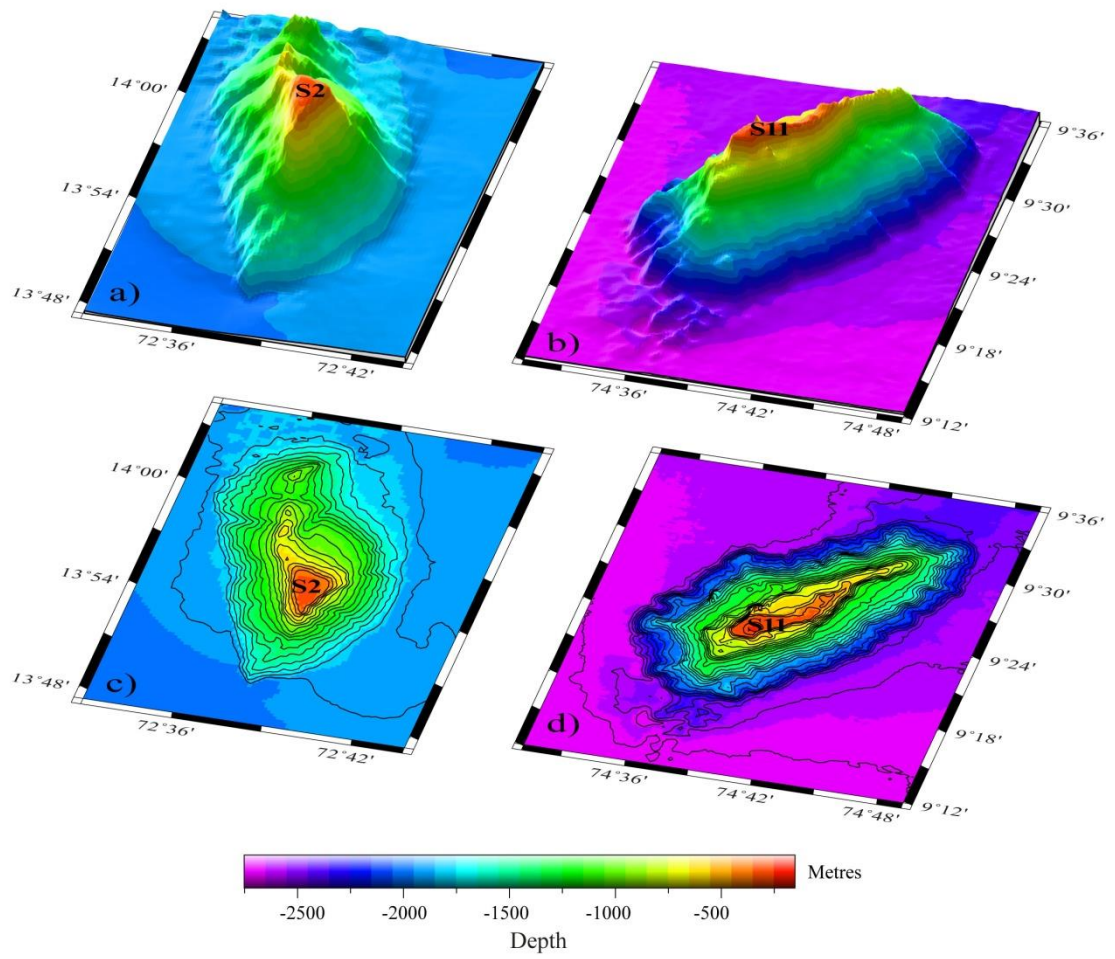


Figure 4

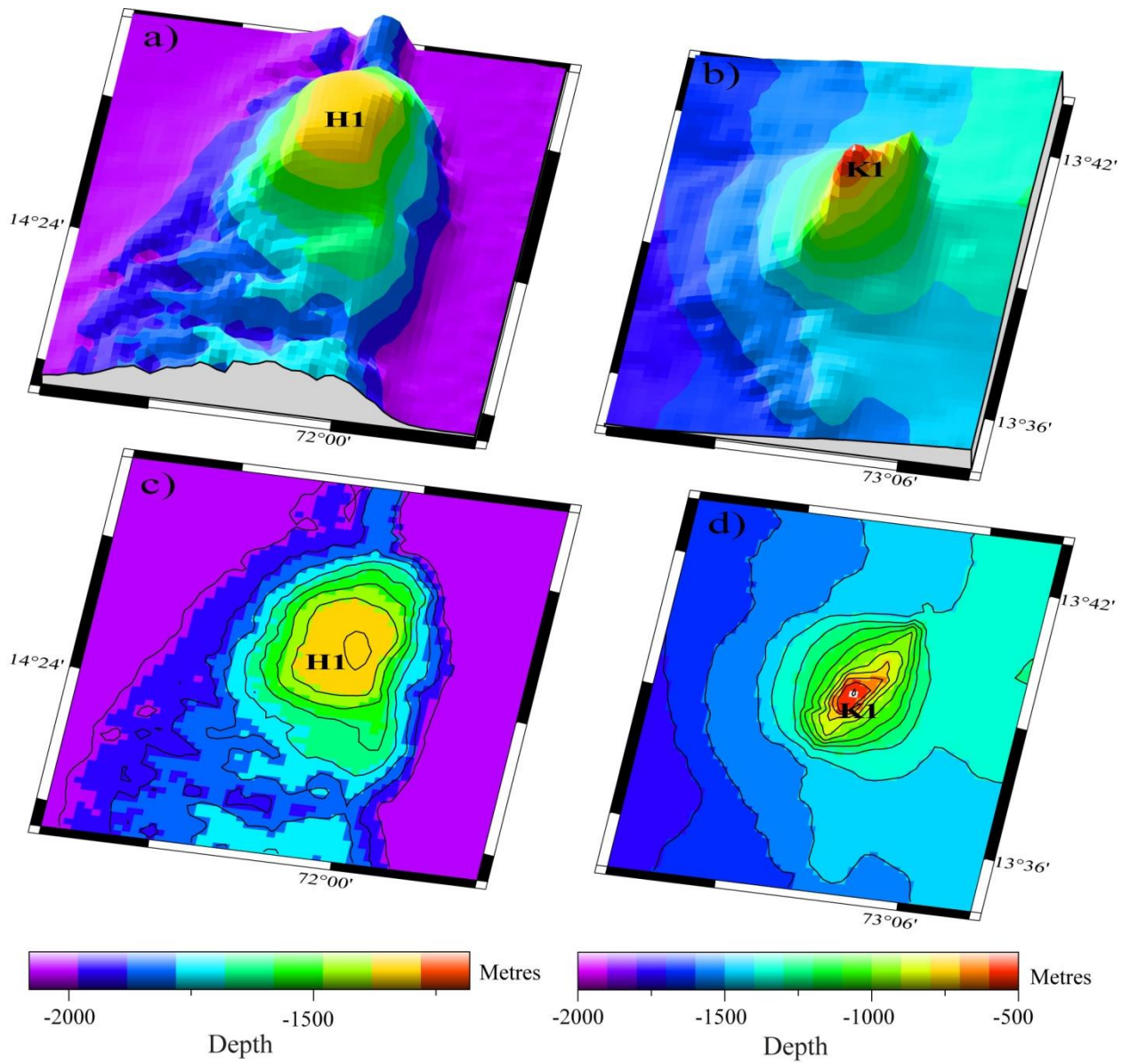


Figure 5

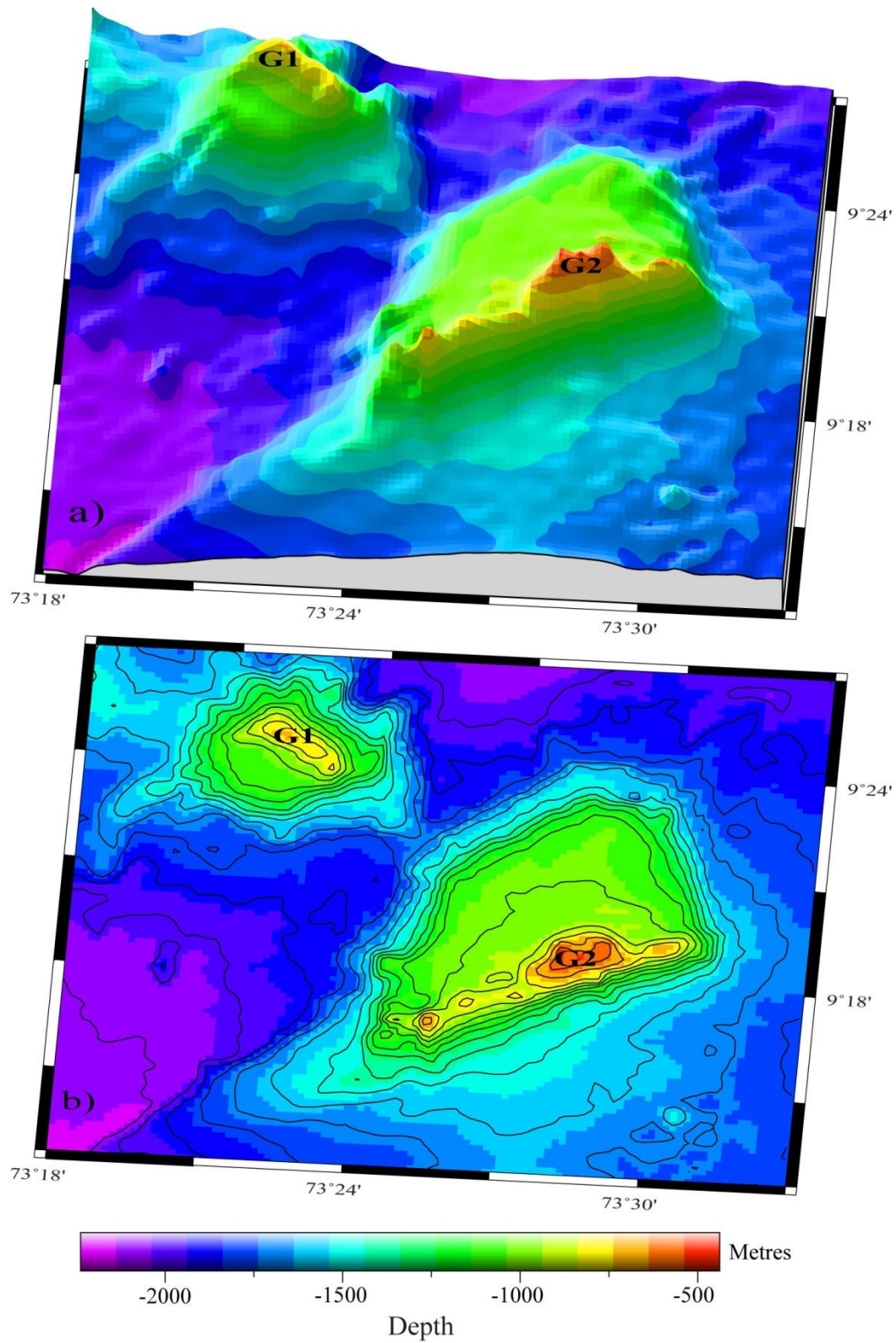


Figure 6

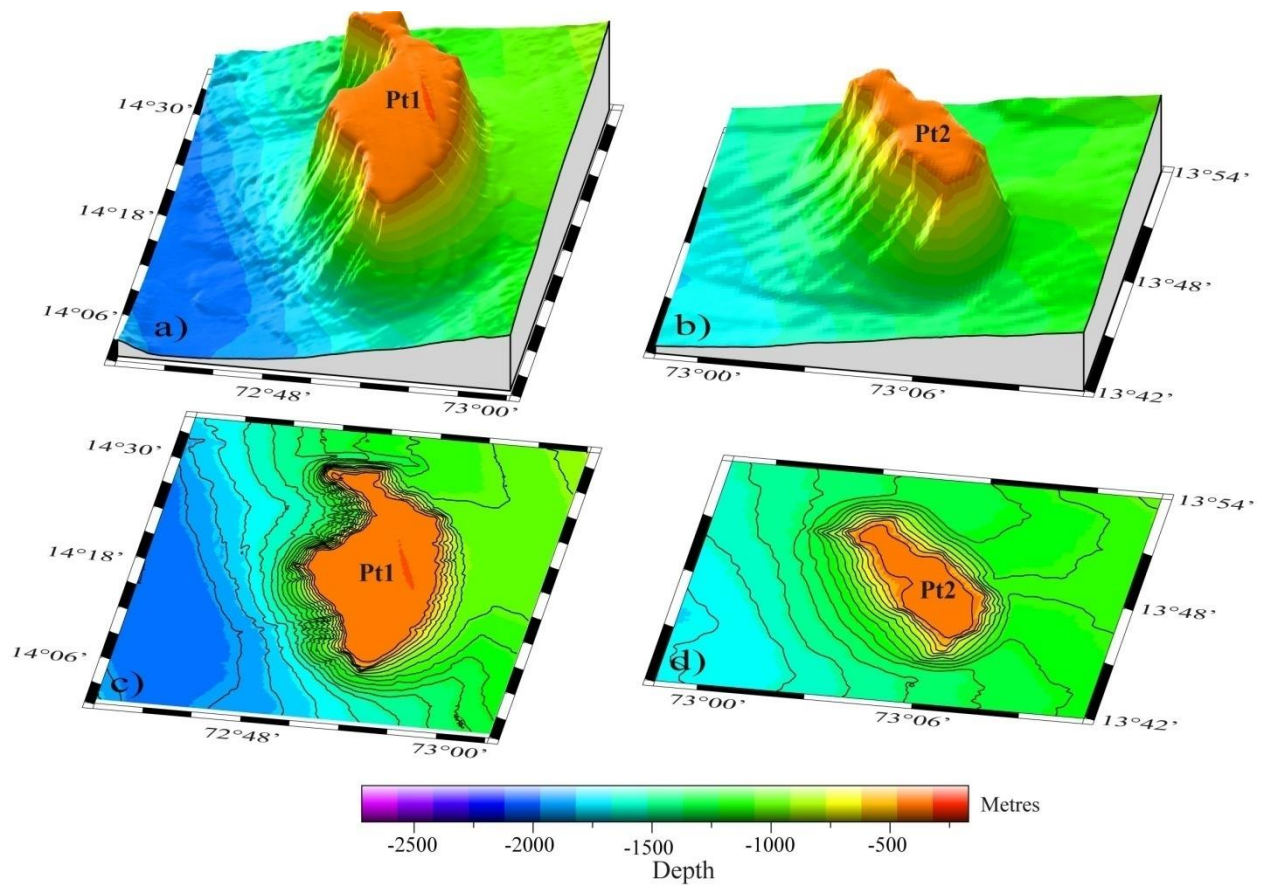


Figure 7

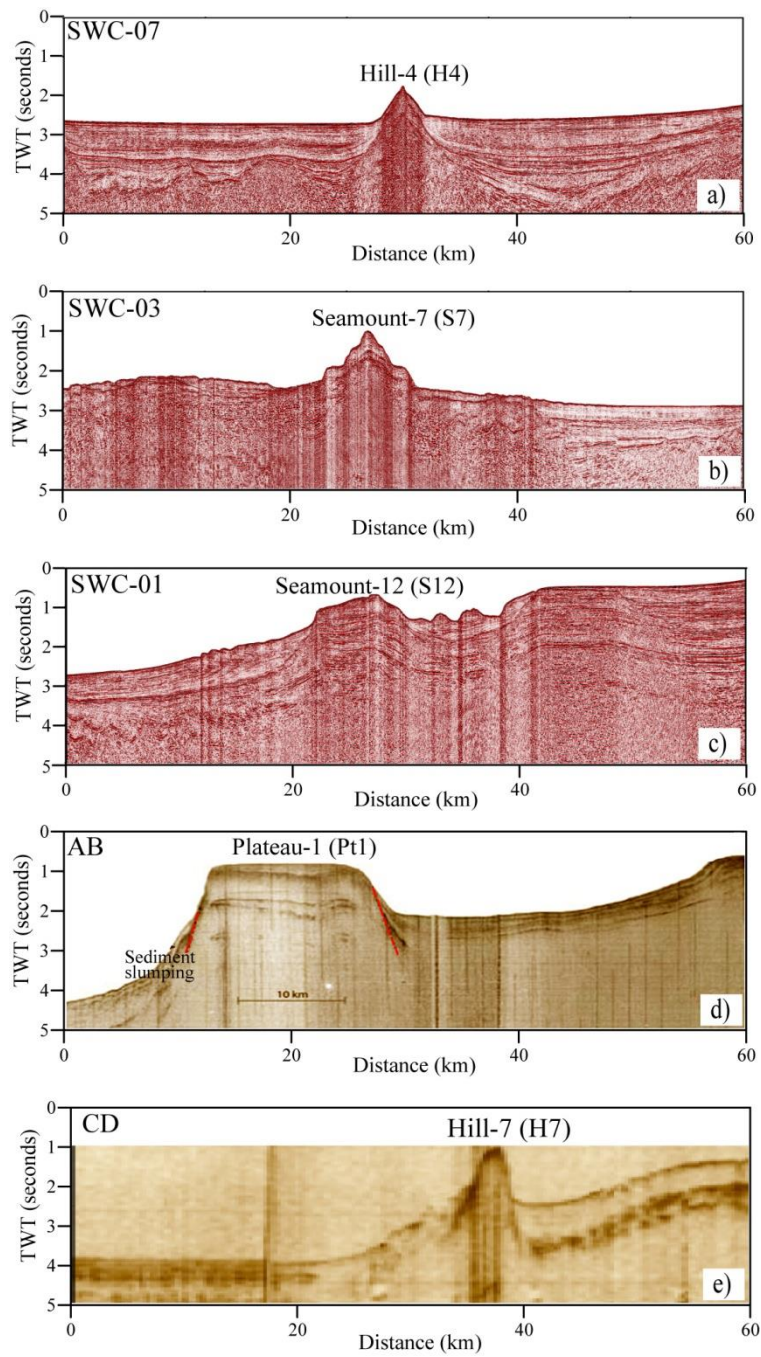


Figure 8

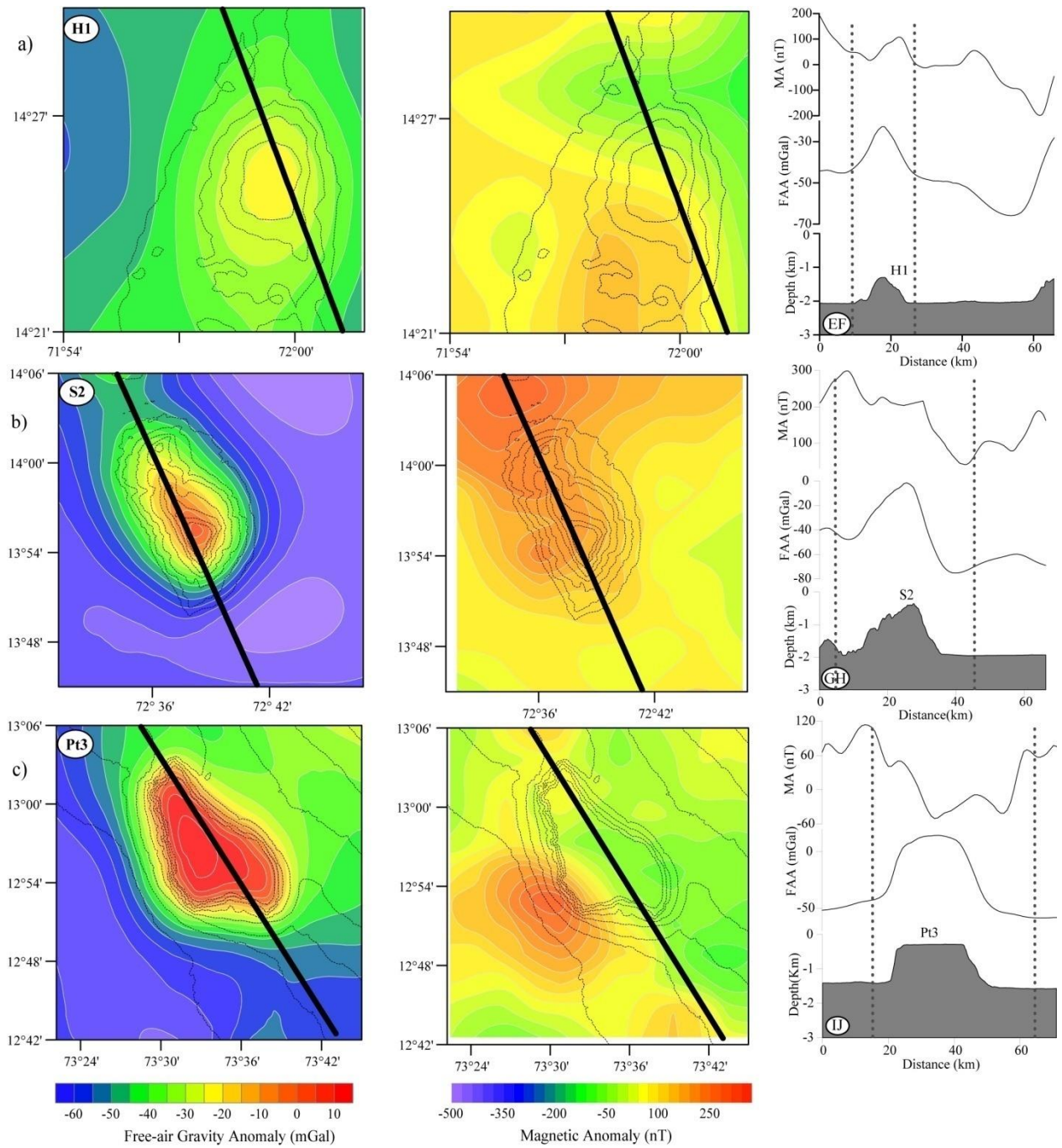


Figure 9

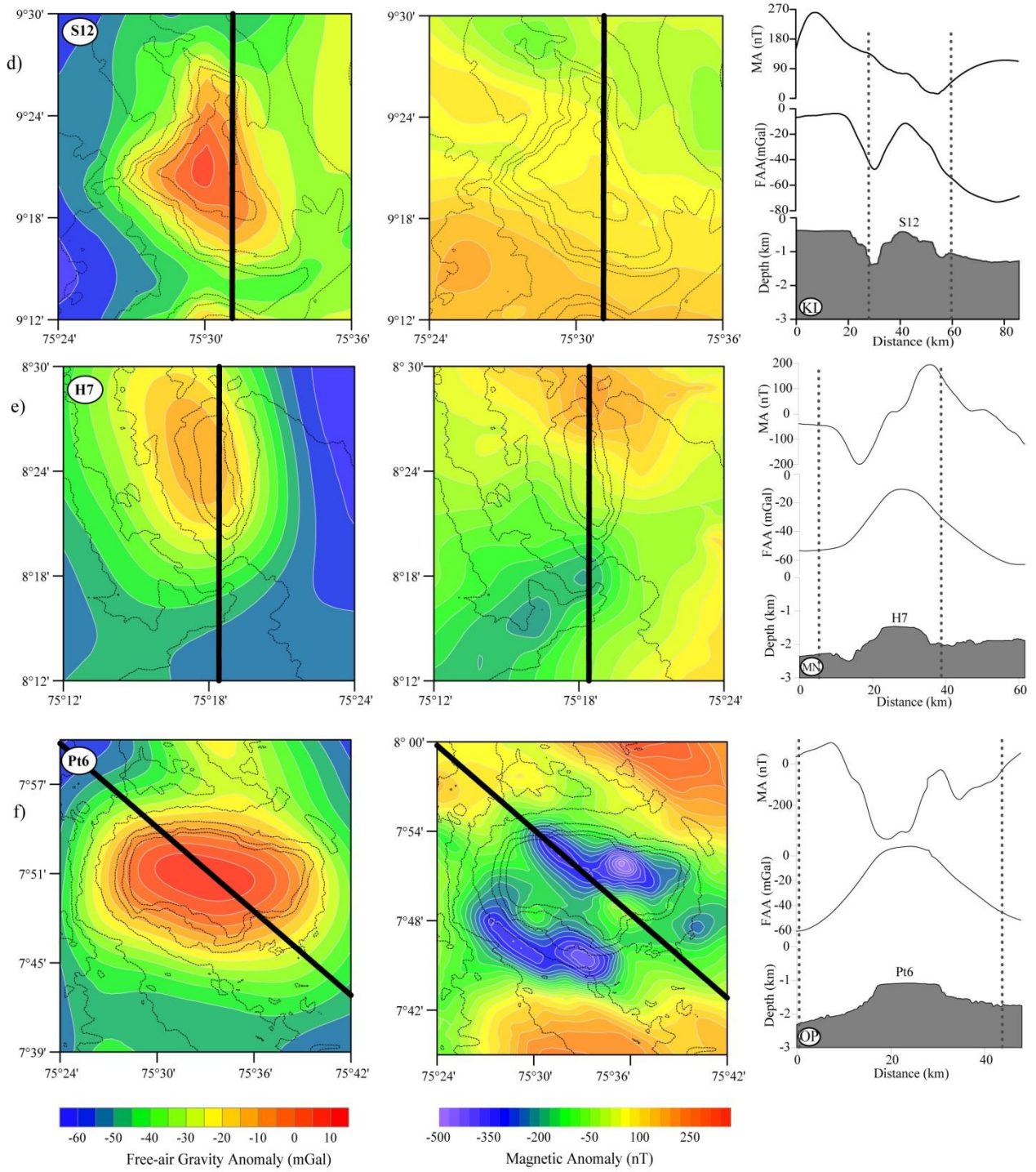


Figure 9 contd.

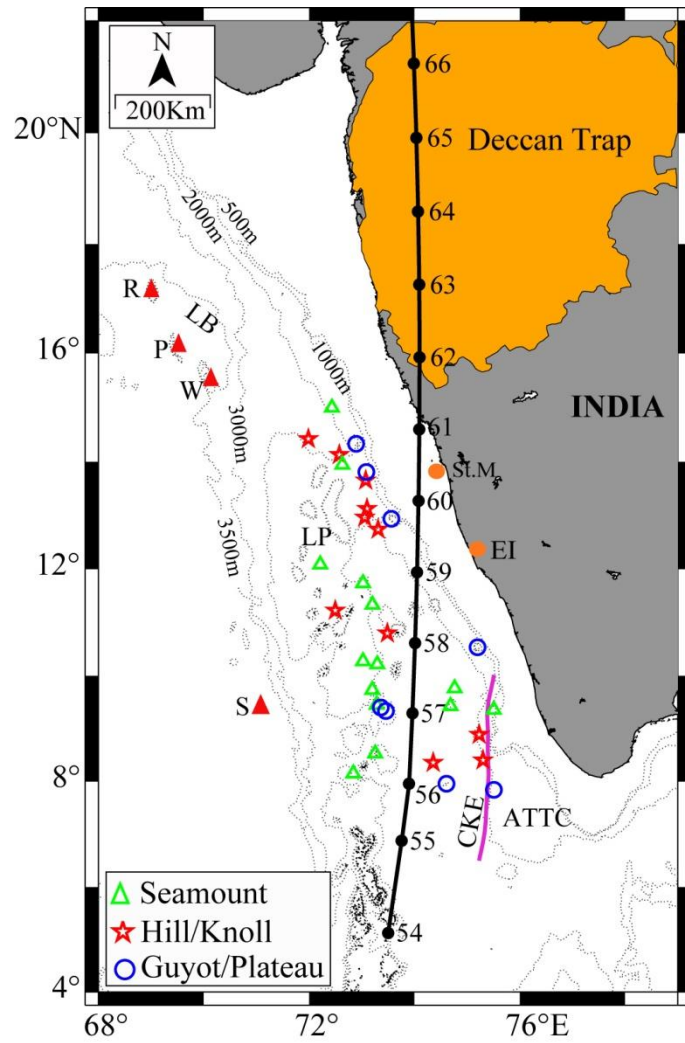


Figure 10

Cruise ID	Vessel	Year	Bathymetry	Gravity	Magnetic
ABP-27	Akademic Boris Petrov	2007	✓	×	×
SK-249	O R V Sagar Kanya	2008	✓	×	×
SK-250	O R V Sagar Kanya	2008	✓	×	×
ABP-33	Akademic Boris Petrov	2008	✓	×	×
SK-257	O R V Sagar Kanya	2009	✓	×	×
SK-275	O R V Sagar Kanya	2010	✓	×	×
ABP-44	Akademic Boris Petrov	2010	✓	×	×
SK-292	O R V Sagar Kanya	2012	✓	×	×
SK-316	O R V Sagar Kanya	2014	✓	×	×
SK-322	O R V Sagar Kanya	2015	✓	×	×
MGS-01	MGS Sagar	2015	✓	✓	×
MGS-02	MGS Sagar	2015	✓	✓	✓
MGS-03	MGS Sagar	2016	✓	✓	✓
MGS-04	MGS Sagar	2016	✓	✓	✓
MGS-06	MGS Sagar	2016	✓	✓	✓
MGS-07	MGS Sagar	2016	✓	✓	✓

Table 1

Feature	Centre Location (DD)	Depth (m)		Height (m) H	Length (km)		Width (km)		Area (sq.km)		H-W ratio (2H/Wb)	Flatness (Ws/Wb)	Average Slope along flanks in degrees	
		Summit	Basal		Summit	Basal	Summit (Ws)	Basal (Wb)	Summit	Basal			East	West
Seamount-1 (S1)	72.433°E, 15.001°N	464	1530	1066	5.26	11.54	1.74	6.65	9.15	76.74	0.321	0.262	8.4	13
Seamount-2 (S2)	72.629°E, 13.943°N	340	1880	1540	5.30	26.70	2.85	13.09	15.11	349.50	0.235	0.218	16.4	18.5
Seamount-3 (S3)	72.212°E, 12.087°N	440	1500	1060	3.82	8.73	0.97	6.10	3.71	53.25	0.348	0.159	11	17
Seamount-4 (S4)	73.022°E, 11.736°N	392	1890	1498	5.48	23.36	2.26	15.79	12.38	368.85	0.190	0.143	11	14
Seamount-5 (S5)	73.201°E, 11.335°N	848	1940	1092	1.30	9.25	0.69	6.04	0.90	55.87	0.362	0.114	10	16
Seamount-6 (S6)	73.023°E, 10.271°N	540	1800	1260	8.40	16.38	2.37	7.43	19.91	121.70	0.339	0.319	14	15
Seamount-7 (S7)	73.294°E, 10.214°N	710	1825	1115	5.20	15.80	0.81	9.27	4.21	146.46	0.241	0.087	14	12
Seamount-8 (S8)	74.763°E, 9.762°N	1265	2310	1045	9.22	27.56	3.95	13.62	36.42	375.36	0.153	0.290	9	10
Seamount-9 (S9)	73.199°E, 9.732°N	300	1935	1635	15.27	40.20	2.35	10.38	35.88	417.27	0.315	0.226	13	19
Seamount-10 (S10)	73.281°E, 9.452°N	895	2210	1315	11.87	34.20	2.73	10.48	32.41	358.41	0.251	0.260	13	17
Seamount-11 (S11)	74.684°E, 9.427°N	240	2500	2260	15.25	34.10	3.1	20.36	47.28	694.27	0.222	0.152	14	12.6
Seamount-	75.504°E,	410	1660	1250	14.34	28.40	3.6	14.05	51.62	399.02	0.178	0.256	10	7.7

12 (S12)	9.357°N													
Seamount-13 (S13)	73.255°E, 8.531°N	208	2097	1889	6.80	40.20	2.48	22.5	16.86	904.50	0.168	0.110	14	17
Seamount-14 (S14)	72.836°E, 8.152°N	362	1790	1428	7.85	17.75	2.55	14.05	20.02	249.38	0.203	0.181	15	5
Hill-1 (H1)	71.985°E, 14.421°N	1290	2020	730	3.58	10.44	1.80	7.94	6.44	82.89	0.184	0.227	14	8.4
Hill-2 (H2)	72.572°E, 14.13°N	1271	1870	599	5.30	10.52	1.76	6.90	9.33	72.59	0.174	0.255	8.5	7.5
Hill-3 (H3)	73.057°E, 12.965°N	1491	1905	414	1.10	5.66	0.30	3.65	0.33	20.65	0.227	0.082	8	4.5
Hill-4 (H4)	73.308°E, 12.740°N	1335	1889	554	1.23	14.83	0.28	4.48	0.34	66.44	0.247	0.063	10	11
Hill-5 (H5)	72.495°E, 11.225°	1010	1760	750	11.20	21.20	7.31	12.50	81.87	265.00	0.120	0.585	12	10
Hill-6 (H6)	75.229°E, 8.888°N	1500	1910	410	7.96	12.50	3.33	5.04	26.51	63.00	0.163	0.661	4	8
Hill-7 (H7)	75.301°E, 8.405°N	1505	2010	505	10.10	18.50	1.50	6.70	151.50	123.95	0.151	0.224	7.7	4.1
Hill-8 (H8)	74.355°E, 8.360°N	2540	2750	210	10.42	23.50	6.29	14.92	65.54	350.62	0.028	0.422	3	2
Knoll-1 (K1)	73.074°E, 13.654°N	490	1430	940	1.70	6.50	0.70	5.10	1.19	33.15	0.368	0.137	19	10
Knoll-2 (K2)	73.098°E, 13.126°N	1508	1820	312	2.60	6.10	1.70	4.13	4.42	25.19	0.151	0.412	8.5	7.5
Knoll-3 (K3)	73.485°E, 10.800°N	810	1740	930	2.02	10.70	0.55	9.35	1.11	100.05	0.199	0.059	8.5	10.5
Guyot-1 (G1)	73.364°E, 9.401°N	720	1810	1090	2.50	9.41	3.38	10.25	8.45	96.45	0.213	0.330	15	11.5
Guyot-2 (G2)	73.462°E, 9.332°N	525	1870	1345	11.2	21.60	7.82	15.32	87.58	330.91	0.176	0.510	11.2	16

Plateau-1 (Pt1)	72.893°E, 14.331°N	325	920	595	35.40	54.30	13.5	21.6	477.90	1172.80	0.055	0.625	5.5	6.5
Plateau-2 (Pt2)	73.088°E, 13.811°N	376	1110	734	11.60	19.00	3.60	6.50	41.76	123.50	0.226	0.553	14.9	10.3
Plateau-3 (Pt3)	73.563°E, 12.938°N	265	1040	775	20.00	31.30	7.48	17.68	149.60	553.38	0.161	0.423	12	11.3
Plateau-4 (Pt4)	75.202°E, 10.537°N	370	746	376	11.65	18.00	6.90	13.90	80.39	250.20	0.054	0.496	12.6	11.8
Plateau-5 (Pt5)	74.609°E, 7.955°N	1888	2720	832	13.40	32.60	4.91	13.64	65.79	444.66	0.122	0.360	13.5	9.5
Plateau-6 (Pt6)	75.511°E, 7.844°N	1080	1670	590	7.10	21.30	17.00	32.70	120.70	696.51	0.036	0.520	6.5	7.7

Table 2

Supplementary Material

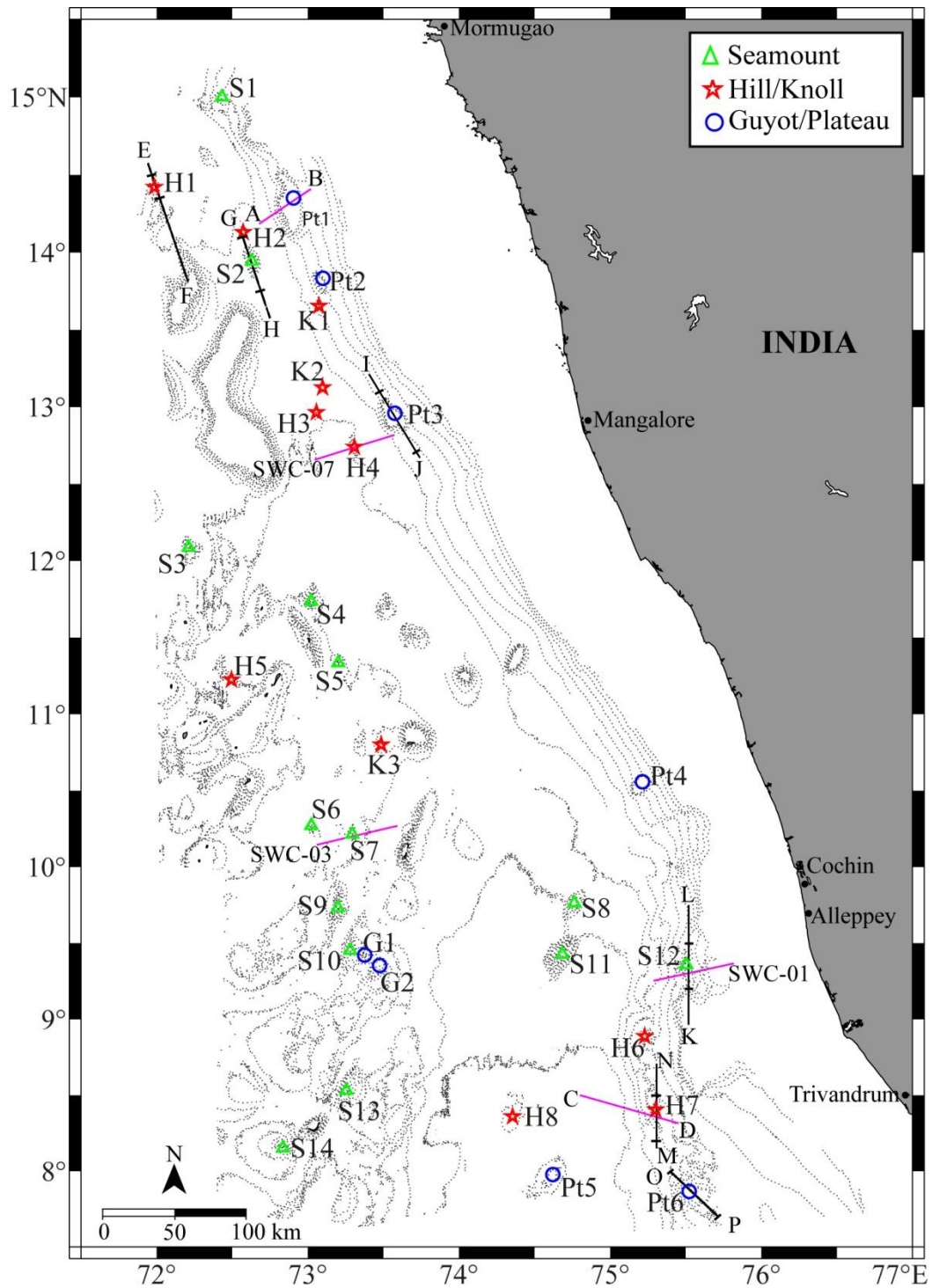
Morphotectonic characteristics, distribution and probable genesis of bathymetric highs off southwest coast of India

C.M. Bijesh, P. John Kurian, V. Yatheesh, Abhishek Tyagi, D. Twinkle

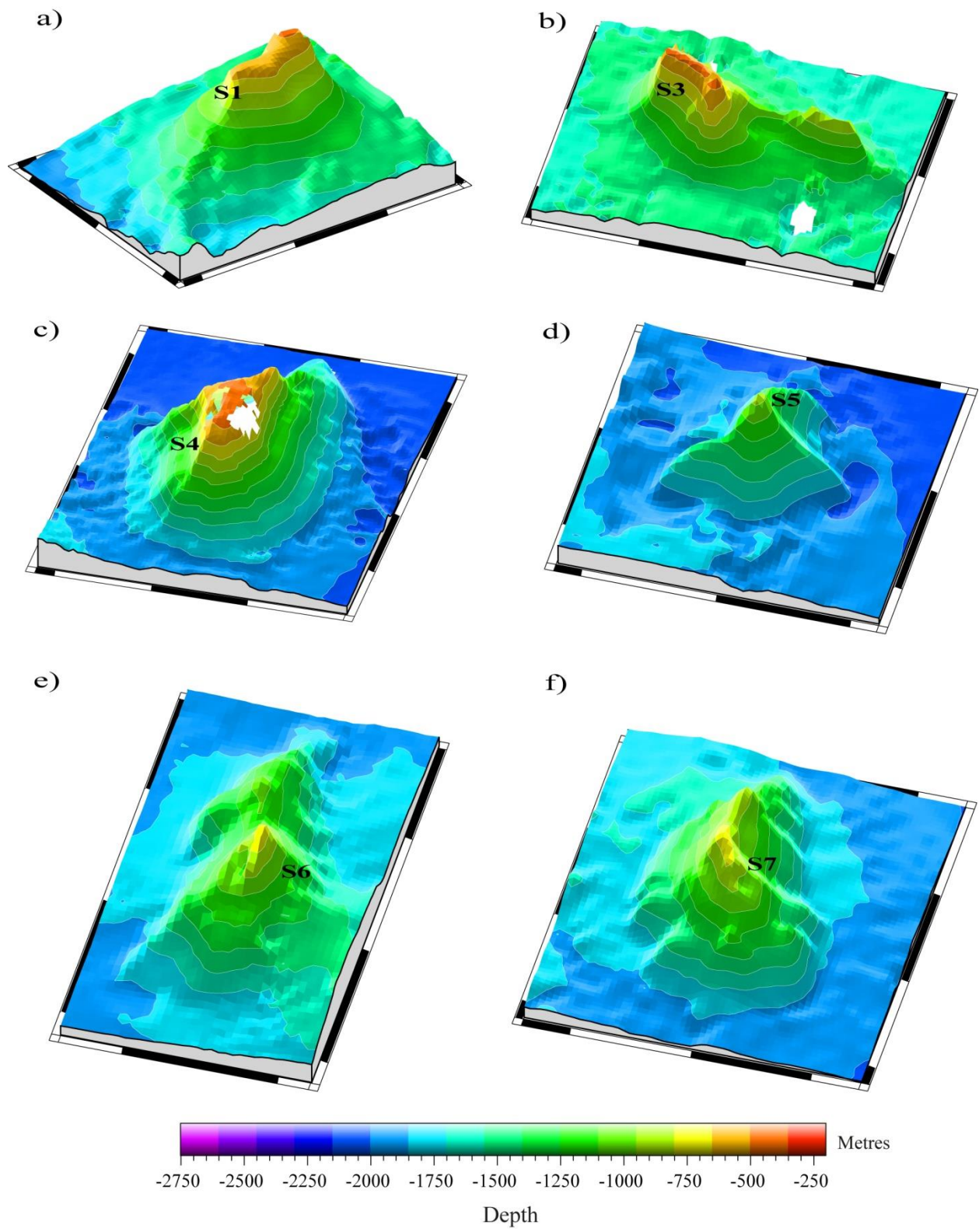
The supplementary material contains five figures which provide detailed information to substantiate the results discussed in the paper.

Captions to Supplementary figures:

Figure S1	The updated high resolution bathymetric map of the study area, showing the locations of the bathymetric high features identified in the present study. Bathymetric contours are in 250 m interval. Pink lines represent locations of the reflection seismic sections presented in Figure 8. Black lines represent locations of sea-surface bathymetry, gravity and magnetic profiles presented in Figure 9 (profile plots). Black cross marks on these lines represent the extent of the profiles shown in Figure 9 (on the colour-coded images). Labels to the bathymetric high features are as in Table 2.
Figure S2	Colour-coded three-dimensional images of the identified seamounts in the study area. (a) Seamount S1; (b) Seamount S3; (c) Seamount S4; (d) Seamount S5; (e) Seamount S6; (f) Seamount S7; (g) Seamount S8; (h) Seamount S9; (i) Seamount S10; (j) Seamount S12; (k) Seamount S13; (l) Seamount S14. White lines indicate isobaths in 150m contour interval.
Figure S3	Colour-coded three-dimensional images of the identified hills in the study area. (a) Hill H2; (b) Hill H3; (c) Hill H4; (d) Hill H5 (e) Hill H6; (f) Hill H7; (g) Hill H8. White lines indicate isobaths in 150m contour interval.
Figure S4	Colour-coded three-dimensional images of the identified knolls in the study area. (a) Knoll K2; (b) Knoll K3. White lines indicate isobaths in 150m contour interval.
Figure S5	Colour-coded three-dimensional images of the identified plateaus in the study area. (a) Plateau Pt3; (b) Plateau Pt4; (c) Plateau Pt5; (d) Plateau Pt6. White lines indicate isobaths in 150m contour interval.

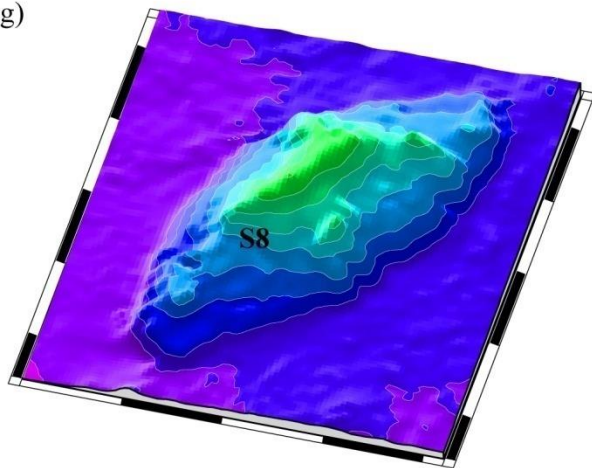


Supplementary Figure S1

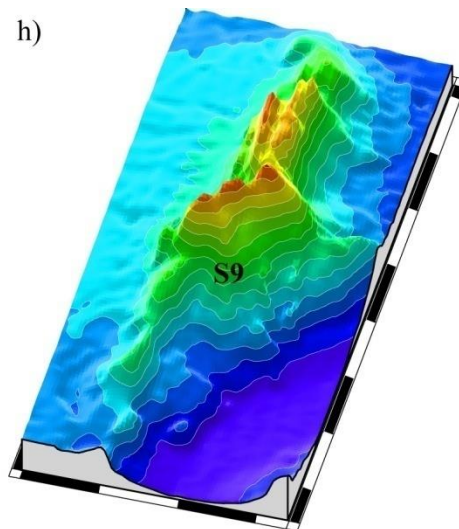


Supplementary Figure S2

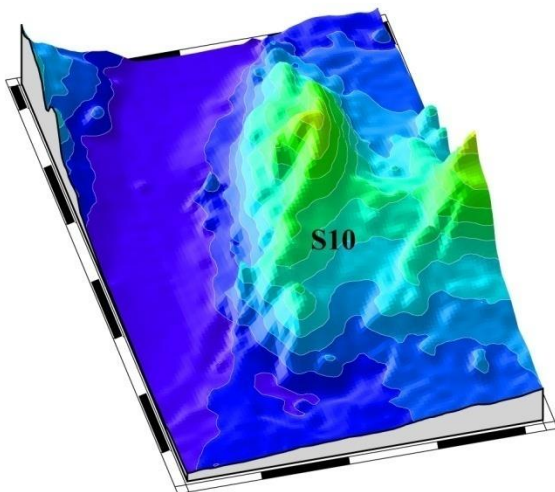
g)



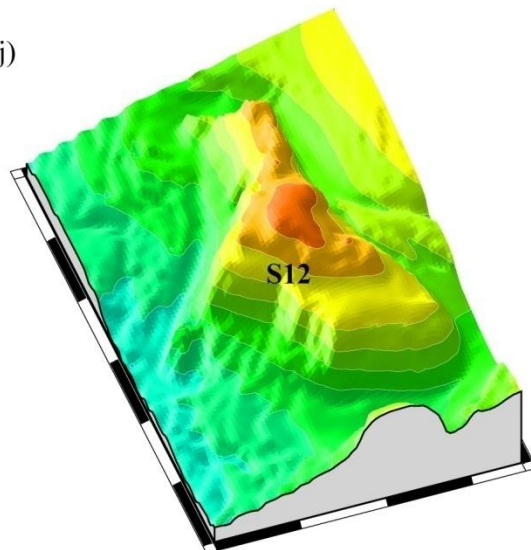
h)



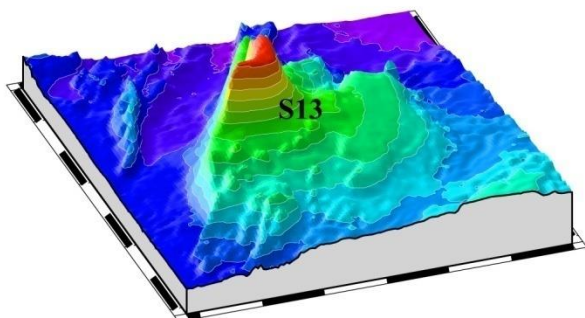
i)



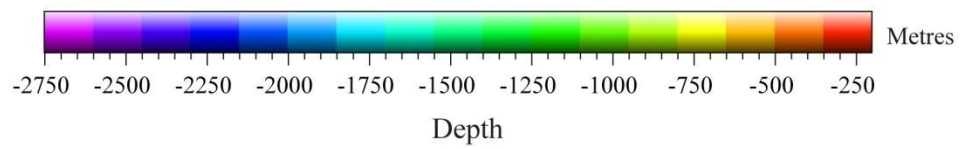
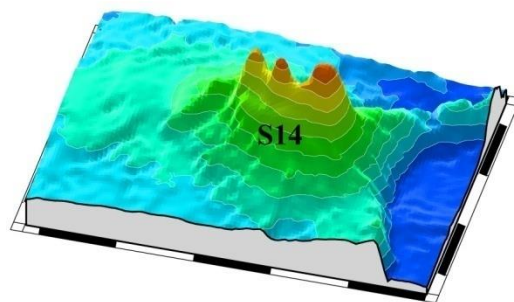
j)



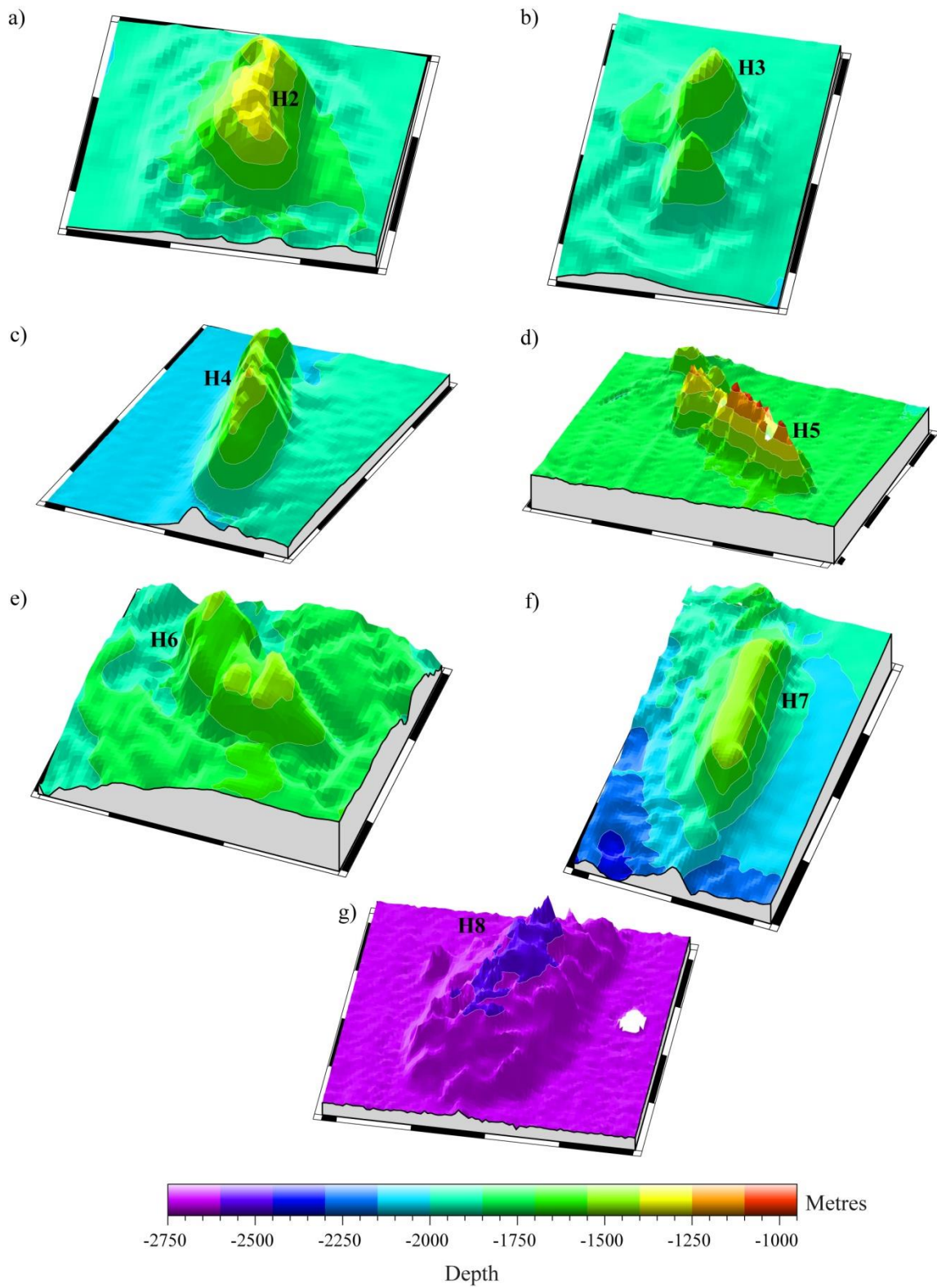
k)



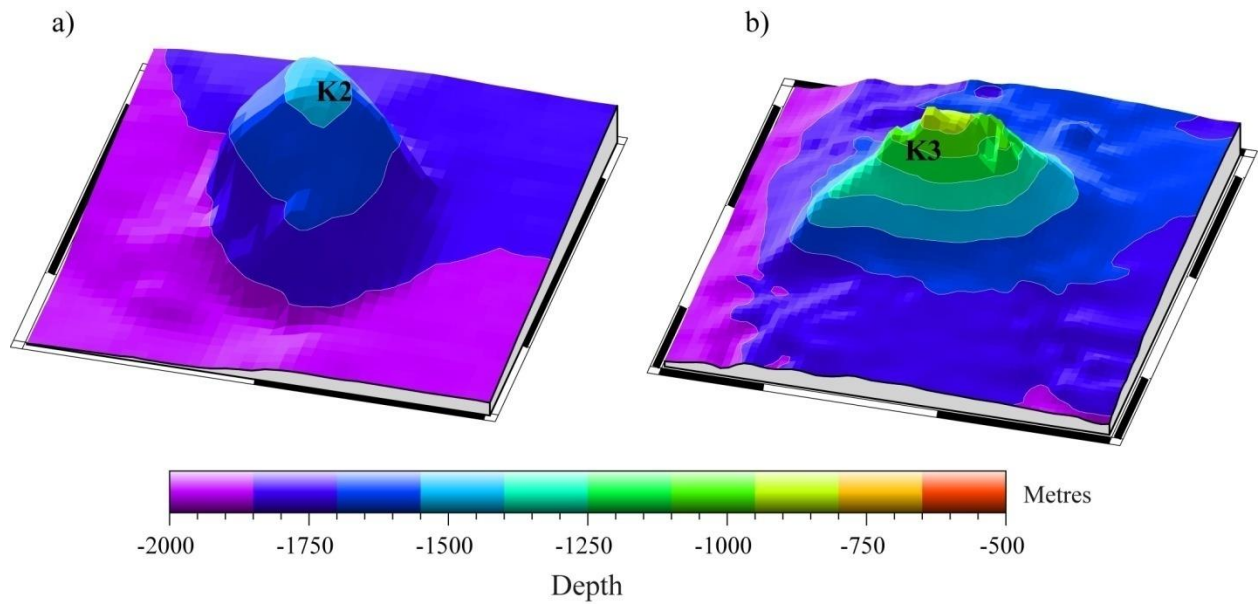
l)



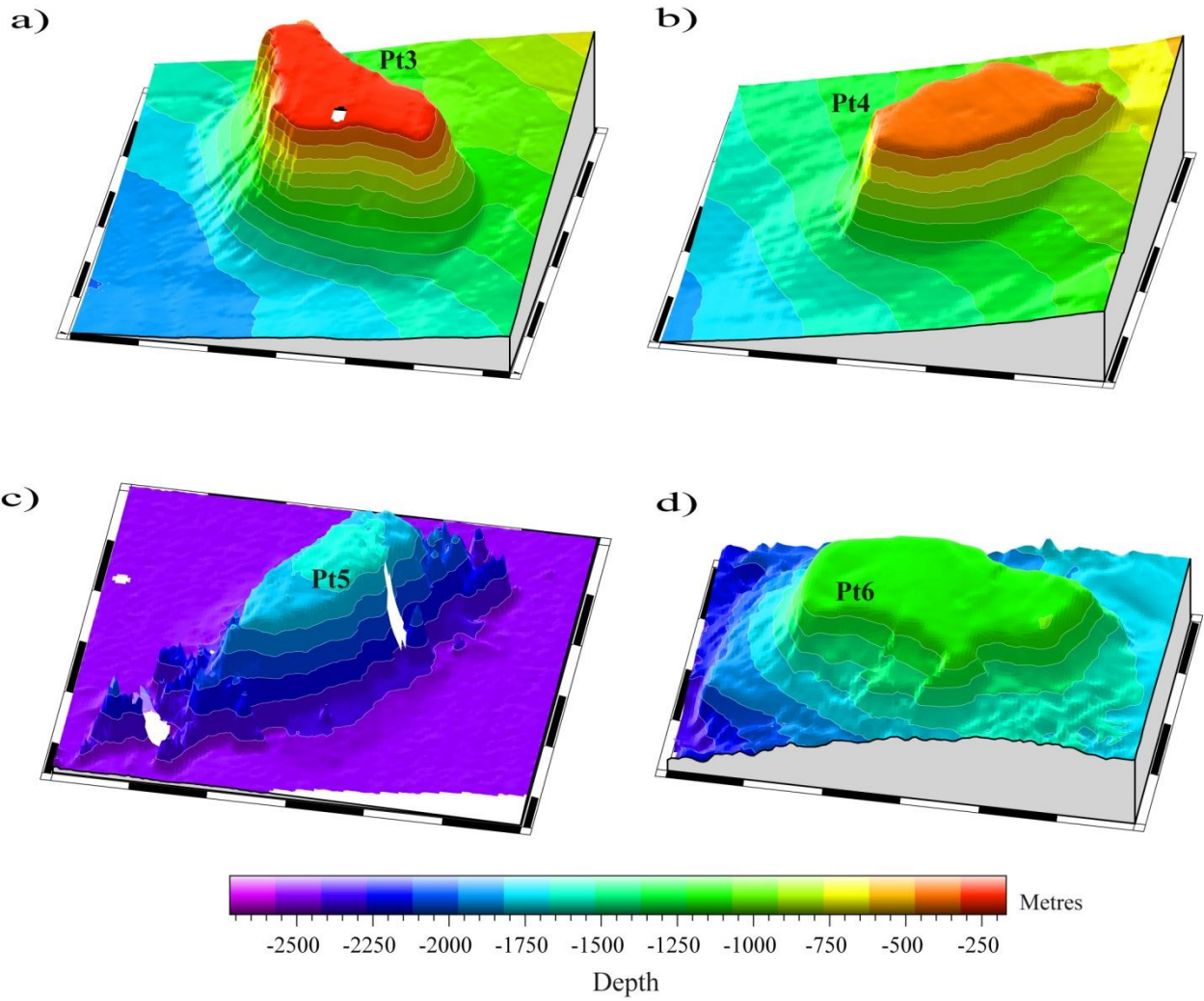
Supplementary Figure S2 Contd.



Supplementary Figure S3



Supplementary Figure S4



Supplementary Figure S5